Investigation and application of thallium isotope fractionation

Sune G. Nielsen[1,2], Mark Rehkämper[3] and Julie Prytulak[3]

[1] - NIRVANA laboratories, Woods Hole Oceanographic Institution, Woods Hole, MA, USA

[2] - Department of Geology and Geophysics, Woods Hole Oceanographic Institution, Woods Hole, MA, USA

[3] - Department of Earth Science and Engineering, Imperial College, London SW7 2AZ, UK

Words: 17052

Figures: 10

Tables: 4

ABSTRACT

This contribution summarizes the current state of understanding and recent advances made in the field of stable thallium (Tl) isotope geochemistry. High precision measurements of Tl isotope compositions were developed in the late 1990s with the advent of multiple collector inductively coupled plasma mass spectrometry (MC-ICPMS) and subsequent studies revealed that Tl, despite the small relative mass difference of the two isotopes, exhibits substantial stable isotope fractionation, especially in the marine environment. The most fractionated reservoirs identified are ferromanganese sediments with $\varepsilon^{205}Tl \approx +15$ and low temperature altered oceanic crust with $\varepsilon^{205}Tl \approx -20$. The total isotopic variability of more than 35 $\varepsilon^{205}Tl$-units hence exceeds the current analytical reproducibility of the measurement technique by more than a factor of 70. This isotopic variation can be explained by invoking a combination of conventional mass dependent equilibrium isotope effects and nuclear field shift isotope fractionation, but the specific mechanisms are still largely unaccounted for.

Thallium isotopes have been applied to investigate paleoceanographic processes in the Cenozoic and there is evidence to suggest that Tl isotopes may be utilized as a monitor of the marine manganese oxide burial flux over million year time scales. In addition, Tl isotopes can be used to calculate the magnitude of hydrothermal fluid circulation through ocean crust. It has also been shown that the subduction of marine ferromanganese sediments can be detected with Tl isotopes in lavas erupted in subduction zone settings as well as in ocean island basalts.

Meteorite samples display Tl isotope variations that exceed the terrestrial range with a total variability of about 50 $\varepsilon^{205}Tl$. The large isotopic diversity, however, is generated by both stable Tl isotope fractionations, which reflect the highly volatile and labile cosmochemical nature of the element, and radiogenic decay of extinct ^{205}Pb to ^{205}Tl with a half-life of about 15 Ma. The

44 difficulty of deconvolving these two sources of isotopic variability restricts the utility of both the
45 ^{205}Pb-^{205}Tl chronometer and the Tl stable isotope system to inform on early solar system
46 processes.
47
48

1. INTRODUCTION

The distribution of Tl in natural environments on Earth is controlled in part by its large ionic radius (Tl^+ = 1.50 A), which is akin to the alkali metals potassium (K), rubidium (Rb) and cesium (Cs) (Heinrichs et al., 1980; Shannon, 1976; Wedepohl, 1974). Thallium's large ionic radius renders it highly incompatible during partial melting and magmatic differentiation, leading to much higher Tl concentrations in the continental crust (Shaw, 1952; Wedepohl, 1995) compared to the mantle (Fig. 1). However, the electron structure of Tl tends to favor covalent bonding, which makes Tl compatible in some sulfides (Genna and Gaboury, 2015; Jones et al., 1993; Kiseeva and Wood, 2013; Nielsen et al., 2011; Nielsen et al., 2014; Wood et al., 2008). In addition to its bonding preferences, Tl has two different valence states: Tl^+ and Tl^{3+}. Although oxidation of Tl requires a large redox potential (Table 1) the manganese (Mn) oxide birnessite has the ability to adsorb and oxidize Tl at its surface (Bidoglio et al., 1993; Peacock and Moon, 2012) and subsequently incorporate Tl^{3+} more firmly in its structure, which leads to very high concentrations of Tl in marine (Fe) Mn oxides (Fig. 1) (Hein et al., 2000; Nielsen et al., 2013; Peacock and Moon, 2012; Rehkämper et al., 2002; Shaw, 1952). Sorption of Tl onto some clay minerals has also been observed (Matthews and Riley, 1970; McGoldrick et al., 1979; Turner et al., 2010) although it is not clear if this behavior is related to the similarity with alkali metals. Thallium's higher particle-reactivity compared to alkali metals results in low concentrations in rivers and the oceans and thus a higher concentration contrast between the ocean and continental crust compared to elements such as Rb, Cs and K (Bruland, 1983; Flegal and Patterson, 1985; Nielsen et al., 2005b).

Thallium has two isotopes with atomic masses 203 and 205 (Table 1) and abundances of ~30% and ~70%, respectively. This equates to a relative mass difference of <1%. Considering

that stable isotope fractionation theory states that the magnitude of isotope fractionation should scale with the relative mass difference of the isotopes (Bigeleisen and Mayer, 1947; Urey, 1947) one would not expect large stable isotope effects for Tl. Hence, it may be surprising that stable isotope investigations for Tl were commenced in the first place. However, the first attempts to measure Tl isotope ratios were not aimed at terrestrial materials. The main reason behind the first Tl isotope studies was the search for potential radiogenic isotope variations due to decay of the now-extinct radioactive isotope ^{205}Pb to ^{205}Tl with a half-life of 15.1 Ma (Pengra et al., 1978), whereas ^{203}Tl is stable and has no radioactive precursor. A number of studies between 1960 and 1994 failed to register resolvable Tl isotope variation for some selected terrestrial and a large number of extraterrestrial materials (Anders and Stevens, 1960; Chen and Wasserburg, 1987, 1994; Huey and Kohman, 1972; Ostic et al., 1969). These investigations were hampered, however, by the relatively large errors (>2‰) associated with the thermal ionization mass spectrometry (TIMS) measurements used at that time. The breakthrough came in 1999 when the first high precision Tl isotope measurements by MC-ICPMS were published (Rehkämper and Halliday, 1999). This technique provided a reduction in the uncertainty of more than an order of magnitude with errors reported at about 0.1-0.2‰ (Rehkämper and Halliday, 1999). With the reduced error bars, analysis of various terrestrial samples revealed large Tl isotope variation in excess of 15 times the analytical reproducibility of the original method, which opened up investigations of Tl isotope fractionation on Earth and in meteorites.

In this contribution, we summarize the knowledge that has been accumulated since 1999 on the stable isotope geochemistry of Tl. Three main environments are discussed: 1) extraterrestrial, 2) the solid Earth, and 3) the marine domain. Throughout these sections, current and notable applications of Tl stable isotopes in geochemical research are incorporated. Finally, potential

95 future studies are suggested that are likely to make Tl isotopes a more quantitative tracer in Earth
96 sciences.
97
98 **2. METHODOLOGY**
99 **2.1. Mass spectrometry**
100 The advent of MC-ICPMS facilitated the development of high-precision Tl isotope ratio
101 measurements. The principal difference to the previous TIMS measurements was the ability to
102 correct for instrumental isotope fractionation that occurs during the measurement (mass bias or
103 mass discrimination). Two-isotope systems are difficult to measure by TIMS because isotope
104 fractionation during volatilization from the filament is both time and mass dependent, which is
105 difficult to correct for. Therefore, precise stable isotope ratios by TIMS are best measured with
106 the use of a double spike (Rudge et al., 2009). However, double spiking can only easily be
107 performed for elements with four or more isotopes (Rudge et al., 2009) and this is the reason
108 why the early Tl isotope studies by TIMS yielded relatively large uncertainties. The great
109 advantage of MC-ICPMS when measuring Tl isotopes (or any two-isotope system) is that, even
110 though the overall magnitude of instrumental mass discrimination is much larger than for TIMS,
111 it can be monitored independently during a measurement and thus corrections can be applied
112 much more precisely than is possible with TIMS. This mass bias correction can be performed
113 because the sample is introduced into the mass spectrometer as a solution (or a desolvated
114 aerosol). Into this solution can be admixed a separate element with a known isotope composition
115 (for Tl this element is Pb) and by assuming that the mass bias incurred for the two elements are
116 proportional, isotope ratios can be determined very accurately and precisely (Nielsen et al., 2004;
117 Rehkämper and Halliday, 1999). For Tl isotope measurements this external normalization with

Pb is always combined with the more conventional standard-sample bracketing technique that is also very common for stable isotope measurements by MC-ICPMS, which produces the most rigorous measurement stability as both instrumental mass bias and machine drift can be corrected for simultaneously. In practice (as is the case for all other stable isotope systems) isotope compositions are conventionally reported by reference to a standard that is defined as zero. For Tl this standard is the NIST 997 Tl metal, such that:

$$\varepsilon^{205}Tl = 10^4 \times (^{205}Tl/^{203}Tl_{sample} - ^{205}Tl/^{203}Tl_{NIST\ 997})/(^{205}Tl/^{203}Tl_{NIST\ 997}) \quad (1)$$

The terminology used for Tl isotope ratios is slightly different from most stable isotope systems, which generally use the δ-notation (variations in parts per 1,000). The reason for this difference is that the Tl isotope system was originally developed as a cosmochemical radiogenic isotope system, which is usually reported using the ε-notation (variations in parts per 10,000). Hence, the original notation was retained in order to facilitate comparisons between cosmochemical and terrestrial data. In addition, the analytical uncertainty on and overall variability of stable Tl isotope ratios make the ε-notation very convenient as most data are thereby shown in whole digits and only a single figure behind the decimal point is needed.

2.2. Chemical separation of thallium

Prerequisites to obtaining precise and accurate stable isotope ratios by MC-ICPMS are the complete separation of the element of interest from the sample matrix as well as 100% recovery. This is important because residual sample matrix in the purified sample can result in isotope effects either present as instabilities that lead to large uncertainties or as reproducible isotopic offsets leading to precise but inaccurate data (Pietruszka and Reznik, 2008; Poirier and Doucelance, 2009; Shiel et al., 2009).

141 The method for separating Tl from sample matrix when performing isotopic analyses of
142 geologic materials was initially developed by Rehkämper and Halliday (1999). The technique
143 has been modified slightly (Baker et al., 2009; Nielsen et al., 2004; Nielsen et al., 2007) from the
144 original recipe, but the fundamentals have remained unchanged. Only the elution procedure has
145 been optimized in order to remove matrix elements most efficiently (Fig. 2). All techniques
146 outlined in Figure 2 achieve effective Tl separation from sample matrix. However, methods that
147 use HBr during matrix elution allow for collection of Pb from the same column, although this
148 procedure has a tendency to separate Pb less efficiently from Tl due to the strong partitioning of
149 bromide-complexed Pb onto anion exchange resin. The separation technique relies on the fact
150 that Tl^{3+} produces anionic complexes with the halogens (the technique uses either Cl^- or Br^-) in
151 acidic solutions that partition very strongly to anion exchange resins. Conversely Tl^+ does not
152 form strong anionic complexes and thus does not partition at all to anion exchange resins.
153 Therefore, samples are prepared in oxidizing media by adding small amounts of water saturated
154 in Br_2 to the samples already digested and dissolved in hydrochloric acid. This process ensures
155 that all Tl is in the trivalent state, which will adsorb onto the anion exchange resin prepared in a
156 quartz or teflon column. If the Tl oxidation was only partial during bromine addition this would
157 cause loss of Tl and likely result in Tl isotope fractionation. However, the procedure routinely
158 produces quantitative recovery of sample Tl (Prytulak et al., 2013), which documents that all Tl
159 is oxidized from bromine addition. The sample matrix can then be eluted in various acidic media
160 as long as Br_2 is present. Lastly, Tl is stripped from the resin by elution with a reducing solution
161 that converts Tl to the univalent state. The reducing solution used is 0.1M hydrochloric acid in
162 which 5% by weight of SO_2 gas has been dissolved. As SO_2 is not stable in solution for long

163 periods of time it is important to make this solution fresh before performing the chemical
164 separation of Tl.
165
166 **2.3. Measurement uncertainties and standards**
167 As with most stable isotope measurements by MC-ICPMS, the smallest uncertainties are
168 obtained for pure standard solutions. The most commonly used secondary standard for Tl is a
169 pure 1,000 μg/g standard solution for ICP-MS concentration analyses that was originally
170 purchased from Aldrich. Over more than 10 years this standard has been measured against NIST
171 997 Tl on seven different mass spectrometers with an average of $\varepsilon^{205}Tl = -0.79 \pm 0.35$ (2sd,
172 n=187). This uncertainty, however, is not necessarily representative of how well samples can be
173 reproduced, mainly because small amounts of sample matrix invariably degrade the
174 measurement precision compared to a pure metal standard even when measuring at the same ion
175 beam intensity. Matrix effects are difficult to quantify and also depend on the sample
176 introduction equipment. However, experiments in which matrix effects were tested by way of
177 doping samples with Tl of a known isotope composition showed no systematic Tl isotope offset
178 due to residual sample matrix (Nielsen et al., 2004). Older studies did find a relationship between
179 sample concentration and measurement uncertainty with the smallest uncertainties obtained for
180 samples with the highest concentrations (Baker et al., 2009; Nielsen et al., 2004; Nielsen et al.,
181 2007; Nielsen et al., 2006a), but the most recent studies have reported external reproducibility
182 for real samples and reference materials that are only slightly worse than what can be achieved
183 for the Aldrich standard (Coggon et al., 2014; Kersten et al., 2014; Nielsen et al., 2015; Prytulak
184 et al., 2013) (Table 2).

In cases where the amount of sample is limited, it can become an important issue how many ions can be measured for a given amount of Tl. Over the last ten years MC-ICPMS instruments have been developed to achieve increased transmission (i.e. the fraction of the ions introduced into the machine that reach the collector) and the most recent instruments have values of >1% for Tl and Pb. This level of transmission routinely produces ion beam intensities of ~20nA for a solution containing 1µg/g Tl and enables Tl isotope analyses on samples as small as 1ng, without notably compromising counting statistics, and an external precision of better than ±1 ε-unit is achievable (Baker et al., 2009; Nielsen et al., 2015; Nielsen et al., 2004; Nielsen et al., 2007; Nielsen et al., 2006a). Smaller sample sizes down to 200pg can still be analyzed on regular Faraday collectors, although precision is significantly degraded to ±3 ε-units (Nielsen et al., 2007; Nielsen et al., 2006a; Nielsen et al., 2009b).

3. THALLIUM ISOTOPE VARIATION IN EXTRATERRESTRIAL MATERIALS

With a half-mass condensation temperature (the temperature at which half of the Tl in the solar nebula was condensed) of 532 K (Lodders, 2003), Tl is classified as a highly volatile element in cosmochemistry. In addition, Tl has also been termed as highly labile (Lipschutz and Woolum, 1988) because it is readily remobilized by processes that are recorded on asteroidal parent bodies and meteroids, including thermal metamorphism and shock heating. Importantly, both properties are conducive to the production of relatively large stable isotope fractionations, and these have been observed for both Tl and other highly volatile elements such as Cd (Wombacher et al., 2008; Wombacher et al., 2003) and Hg (Lauretta et al., 1999; Lauretta et al., 2001) in various extraterrestrial materials.

3.1. The ^{205}Pb–^{205}Tl decay system

The radiogenic Tl isotope variations recorded in meteorites reflect decay of the short-lived radionuclide ^{205}Pb to ^{205}Tl with a half-life of 15.1 Ma (Pengra et al., 1978). Interest in the ^{205}Pb–^{205}Tl decay system and the initial solar system abundance of ^{205}Pb was responsible for driving the first efforts to precisely determine the Tl isotope compositions of natural materials. In detail, the literature documents six attempts to identify radiogenic Tl isotope variations in iron meteorites and chondrites from 1960 to 1995 (Anders and Stevens, 1960; Arden and Cressey, 1984; Chen and Wasserburg, 1987, 1994; Huey and Kohman, 1972; Ostic et al., 1969). Whilst these studies were able to provide an upper limit for the initial solar system ^{205}Pb abundance they were unable to conclusively establish radiogenic Tl isotope variations from the decay of this now-extinct nuclide.

The strong historic interest in the ^{205}Pb–^{205}Tl decay system stems from studies of stellar nucleosynthesis, which indicate that ^{205}Pb is produced primarily or almost exclusively by s-process nucleosynthesis (Blake et al., 1973; Wasserburg et al., 2006; Wasserburg et al., 1994; Yokoi et al., 1985), whereby heavier elements are formed by slow neutron capture in the interior of stars. For astrophysicists, precise constraints on the initial solar system abundance of ^{205}Pb, gained from analyses of meteorites, would hence offer unique clues on the site and operation of s-process nucleosynthesis and the extent to which this process contributed to the freshly synthesized nucleosynthetic material that was delivered to the nascent solar system. In addition, the ^{205}Pb–^{205}Tl decay system is also of interest as a chronometer of volatile depletion as well as core formation and cooling. The latter applications follow from the observation that Pb/Tl ratios are likely to be fractionated by both processes, as (i) Pb, with a half-mass condensation temperature of 727 K (Lodders, 2003), is somewhat less volatile than Tl and (ii) Pb and Tl

exhibit different extents of moderately siderophile and chalcophile affinity during metal-sulfide-silicate partitioning (Ballhaus et al., 2013; Jones et al., 1993; Wood et al., 2008).

Despite of the numerous potential applications, only relatively few Tl isotope studies of meteorites have been attempted using the much more precise MC-ICP-MS methods which superseded TIMS measurements following the pioneering study of Rehkämper and Halliday (1999). These investigations were all motivated by the ^{205}Pb–^{205}Tl chronometer but resolved both radiogenic and stable Tl isotope variations in various stony and iron meteorites. A summary of this work, key results, and cosmochemical implications are presented below.

3.2. Chondritic meteorites

3.2.1. Carbonaceous chondrites

Baker et al. (2010b) carried out a comprehensive study of 10 carbonaceous chondrites of groups CI1 (Orgueil), CM2 (incl. Murchison), CR2, CV3 (incl. Allende), and CO3. Two samples were excluded from the evaluation of radiogenic Tl isotope effects as they had fractionated Cd isotope compositions due to thermal processing (Wombacher et al., 2008; Wombacher et al., 2003), and this may have also affected Tl isotopes, whilst four samples were corrected for terrestrial Pb contributions of between 9 and 77% of total Pb, based on measured Pb isotope data.

Overall, the Tl and Pb concentrations of the meteorites varied by more than a factor of 5, between about 20 ng/g (in CR2 chondrites) to 100 ng/g (in Orgueil CI1) for Tl and 340 to 2200 ng/g for Pb. Importantly, the results showed a clear co-variation between Tl and Pb, which was used to derive average carbonaceous chondrite and, by inference, solar system Pb/Tl and ^{204}Pb/^{203}Tl ratios of 22±2 and 1.43±0.14 respectively (uncertainties are 2sd).

253 Furthermore, the samples revealed a small but significant correlated variability between Tl
254 isotope compositions, with ε^{205}Tl values of −4.0 to +1.2, and ^{204}Pb/^{203}Tl ratios (Fig. 3). A
255 number of observations, in particular unfractionated stable Cd isotope compositions in all the
256 samples, indicate that this correlation is unlikely to be due to stable isotope fractionation from
257 early solar system processes or terrestrial weathering, and is instead most readily explained by in
258 situ decay of ^{205}Pb to ^{205}Tl. Previous ^{53}Mn–^{53}Cr and ^{107}Pd–^{107}Ag studies of bulk carbonaceous
259 chondrites furthermore suggest that the Pb–Tl isochron records volatile fractionation in the solar
260 nebula at close to 4567 Ma (Schönbächler et al., 2008; Shukolyukov and Lugmair, 2006). If this
261 interpretation is correct, then the isochron of Fig. 3 yields the initial ^{205}Pb abundance and Tl
262 isotope composition of the solar system, with values of $^{205}Pb/^{204}Pb_{SS,0} = (1.0\pm0.4)\times10^{-3}$ and
263 $\varepsilon^{205}Tl_{SS,0} = -7.6\pm2.1$, respectively. These results provide clear evidence for the existence of live
264 ^{205}Pb in the early solar system. The inferred $^{205}Pb/^{204}Pb_{SS,0}$ ratio is close to the upper limit of
265 nucleosynthetic production estimates for AGB stars (Wasserburg et al., 2006) and thus in accord
266 with contributions of such stars to the early solar system budget of freshly synthesized
267 nucleosynthetic matter.
268
269 *3.2.2. Enstatite chondrites*
270 Analyses were carried out on a suite of enstatites chondrites, comprised of three less
271 metamorphosed samples from groups EL3, EH4 and three equilibrated meteorites from groups
272 EH5 and EL6 (Palk et al., 2011). In detail, the EL3 and EH4 enstatite chondrites were found to
273 have much higher volatile contents (of about 40 to 100 ng/g Tl) than the intensely
274 metamorphosed samples of groups EH5 and EL6, which had Tl abundances of only about 5 ng/g
275 Tl. Whilst four of the meteorites displayed moderate to extreme Cd isotope fractionations of up

276 to $\varepsilon^{114/110}$Cd ≈ +70, only a single sample displayed a clearly fractionated Tl isotope composition
277 with ε^{205}Tl ≈ +22. As this sample is known to be highly shocked (with a grade of S5), it is
278 possible that Tl was mobilized and isotopically fractionated during shock metamorphism.
279 In contrast, all other enstatite chondrites yielded a narrow range of ε^{205}Tl values, with results
280 of between –2.9 and +0.8. Given the limited isotopic variability, the observation of Tl (and more
281 prevalent Cd) stable isotope fractionation, and the presence of terrestrial Pb contamination (in
282 two meteorites) as revealed by Pb isotopes, a robust Pb-Tl isochron could not be obtained for the
283 enstatite chondrites.
284
285 *3.2.3. Ordinary chondrites*
286 Only a single Pb-Tl study of ordinary chondrites has been attempted, with results reported
287 for samples of groups L and LL (Andreasen et al., 2009). To minimize the problem of terrestrial
288 Pb contamination, only meteorite falls were selected for analysis. Overall, these meteorites
289 displayed a large spread in ^{204}Pb/^{203}Tl ratios from 1.7 to 152, as a result of large variations in Tl
290 concentration (from 0.3 to 19 ng/g), whilst Pb abundances varied by less than a factor of 7. The
291 Tl isotope compositions were also highly variable with ε^{205}Tl values of between about -20 to
292 +15.
293 Given the observation of large Cd isotope fractionations in ordinary chondrites (Wombacher
294 et al., 2008; Wombacher et al., 2003), the Tl isotope variability was assessed to distinguish
295 radiogenic effects from clearly evident mass dependent Tl isotope fractionations, presumably
296 from mobility and redistribution of Tl during thermal metamorphism. Consequently, the
297 equilibrated LL and L chondrites (of type 4-6) were judged to show no evidence of radiogenic
298 ^{205}Tl, indicating that the high Pb/Tl ratios were established by elemental redistribution after ^{205}Pb

299 was extinct. In contrast, the Tl isotope compositions of unequilibrated LL3 chondrites were
300 interpreted to reflect radiogenic ingrowth of ^{205}Tl, with a Pb-Tl age of about 45 Ma after solar
301 system formation.
302
303 **3.3. Iron meteorites**
304 Due to the relatively high volatile element contents, IAB irons are the most straightforward
305 iron meteorites for Tl isotope and Pb-Tl isochron analyses. Such measurements were also
306 conducted for IIAB and IIIAB irons, but are significantly more difficult as much larger samples
307 (generally more than 15 g; Nielsen et al. (2006a)) are required to obtain robust Tl isotope data
308 and because the nearly ubiquitous terrestrial Pb contamination is more problematic due to the
309 low meteoritic Pb contents. No data are currently available for the even more volatile depleted
310 irons of groups IVA and IVB.
311
312 *3.2.1. Non-magmatic IAB complex iron meteorites*
313 Nielsen et al. (2006a) analyzed seven metal samples and five troilite nodules of the IAB
314 main group irons Toluca and Canyon Diablo. The metal samples had Tl concentrations from
315 about 0.03 ng/g to 16.5 ng/g and variable $^{204}Pb/^{203}Tl$ from about 0.1 to more than 75, equivalent
316 to Pb/Tl ratios of between about 2 and 1200. Notably, the Tl isotope compositions, which ranged
317 between $\varepsilon^{205}Tl$ values of about -3 to +23 were observed to correlate with $^{204}Pb/^{203}Tl$ (Fig. 4).
318 When interpreted as an isochron, this correlation corresponds to initial values of $^{205}Pb/^{204}Pb_0$ =
319 $(7.3\pm0.9) \times 10^{-5}$ and $\varepsilon^{205}Tl_0 = -2.2\pm1.5$. Alternative explanations for the correlation, such as
320 mixing of variably mass fractionated meteorite components or terrestrial contamination are
321 difficult to reconcile with the results. Troilite nodules from Toluca and Canyon Diablo contain Tl
322 that is generally significantly less radiogenic than the co-existing metal with isotope

compositions that are variable and decoupled from $^{204}Pb/^{203}Tl$ (Fig. 4). These effects were interpreted to result from kinetic stable isotope fractionation during diffusion of Tl between metal and sulfide. Given the relatively low Tl contents of the troilites (with about 1.6 to 27 ng/g Tl) and the low overall abundance of sulfides in IAB irons (≤2% of mass), such processes are unlikely to have significantly affected the Tl isotope compositions of the co-existing metal.

Assuming a solar system initial $^{205}Pb/^{204}Pb_{SS,0} = (1.0\pm0.4)x10^{-3}$, as derived from carbonaceous chondrites (Fig. 3), the IAB isochron was established 57 +10/−14 Ma after the start of the solar system (Baker et al., 2010b). In comparison, recent Pd–Ag isochron studies of the same meteorite groups indicate that the Pd-Ag fractionation of IAB irons is only about 15 to 19 Ma younger than carbonaceous chondrites (Carlson and Hauri, 2001; Schönbächler et al., 2008; Theis et al., 2013; Woodland et al., 2005). The Pb–Tl and Pd–Ag ages are thus only barely consistent, within the combined uncertainties, hinting at possible discrepancies between the two ages. Most likely, the relatively young Pb–Tl isochron age of the IAB metals reflects late closure of this isotope system, due to a blocking temperature that is significantly lower than the 1100 K blocking temperature of the Pd-Ag chronometer (Sugiura and Hoshino, 2003) and possibly similar to that of the K–Ar system at 650 K (Renne, 2000; Trieloff et al., 2003). This interpretation is in accord with the highly labile nature of Tl, as opposed to Ag, during thermal processing (Lipschutz and Woolum, 1988).

Also not in accord with the IAB isochron are the results obtained for the anomalous IAB complex iron Mundrabilla (Fig. 4; (Nielsen et al., 2006a)). Two metal samples and a sulfide nodule of this meteorite were characterized by $\varepsilon^{205}Tl$ values of about +30 and +24, respectively. It is likely that the high $\varepsilon^{205}Tl$ found in Mundrabilla is not solely due to rapid radiogenic ingrowth of ^{205}Tl in a high Pb/Tl environment but also reflects, at least in part, significant stable

346 isotope fractionations, most likely associated with volatile loss from or redistribution on the
347 parent body.
348
349 *3.3.2. Magmatic IIAB and IIIAB iron meteorites*
350 Andreasen et al. (2012) conducted a comprehensive Pb-Tl isochron study of metal samples
351 from six IIAB and six IIIAB iron meteorites. All samples were thoroughly leached prior to
352 dissolution to remove terrestrial Pb contamination. The fraction of primordial Pb was then
353 calculated by assuming that any deviation in the Pb isotope composition of the iron meteorites
354 from primordial Pb is due to residual contributions from terrestrial Pb. The meteorite samples
355 exhibited low and highly variable Tl contents ranging from 0.002 to 0.485 ng/g, with most Tl
356 concentrations at less than 0.02 ng/g. The IIAB and IIIAB iron meteorites are hence, on average,
357 significantly more depleted in Tl than the IAB irons.
358 The $^{204}Pb/^{203}Tl$ ratios of the meteorites (Fig. 5, (Andreasen et al., 2012)) varied from 0.05 to
359 5.8 for the IIAB irons (Pb/Tl ≈ 0.8 to 89) and from 1.6 to 14 for the IIIABs (Pb/Tl ≈ 26 to 215).
360 As such, these magmatic irons have $^{204}Pb/^{203}Tl$ ratios that are noticeably less variable than in
361 IABs (Fig. 4), and with many samples not far removed from the chondritic value of $^{204}Pb/^{203}Tl$ =
362 1.43 (Pb/Tl = 22). The $\varepsilon^{205}Tl$ values of the IIAB and IIIAB irons ranged from –18 to +23 (Fig.
363 5). The majority of the Tl isotope data, furthermore, display a correlation of $\varepsilon^{205}Tl$ with
364 $^{204}Pb/^{203}Tl$, suggesting that the isotopic variations are primarily governed by decay of ^{205}Pb at
365 variable Pb/Tl ratios.
366 Further Pb-Tl analyses for metal samples from two IIAB and two IIIAB irons and a IIIAB
367 troilite nodule were reported by Nielsen et al. (2006a). For the IIABs, these data do not support
368 the IIAB errorchron inferred by Andreasen et al. (2012) (Fig. 5). It is possible that this

discrepancy arises, at least in part, from the less accurate correction of residual terrestrial Pb contamination that was utilized by Nielsen at al. (2006a) or possibly even minor terrestrial Tl contributions. Alternatively, the non-isochronous behavior of the IIABs analyzed by Nielsen at al. (2006a) may reflect late open system behavior and/or stable isotope fractionation of Tl in some samples. In contrast, the two IIIAB metals and the IIIAB troilite analyzed by Nielsen et al. (2006a) yield results, which are in accord with the IIIAB isochron reported by Andreasen et al. (2012) (Fig. 5).

Assuming that the IIAB data of Andreasen et al. (2012) indeed define a Pb-Tl isochron (Fig. 5), they correspond to an initial $^{205}Pb/^{204}Pb_0$ ratio of $(8.3\pm1.6)\times10^{-4}$. This ^{205}Pb abundance is equivalent to an age of 4 +16/-14 Ma, assuming an initial solar system abundance of $^{205}Pb/^{204}Pb_{SS,0} = (1.0\pm0.4)\times10^{-3}$, as defined by carbonaceous chondrites (Fig. 3) (Baker et al., 2010b). A similar but more uncertain initial ^{205}Pb abundance and a less well-constrained age of 4 +29/-14 Ma was obtained from the IIIAB correlation (Fig. 5). Both iron meteorite isochrons, however, have y-intercepts with initial $\varepsilon^{205}Tl_0$ values that are more negative (at $\varepsilon^{205}Tl_0 = -12\pm1$ for the IIABs) than the initial solar system value of $\varepsilon^{205}Tl_{SS,0} = -7.6\pm2.1$, as defined by the carbonaceous chondrites isochron (Fig. 3). It is conceivable that the observed offset of about 7 ε-units (at the chondritic value of $^{204}Pb/^{203}Tl = 1.43$) between the IIAB and the chondrite isochron reflects a nucleosynthetic isotope anomaly or is caused by stable Tl isotope fractionation. However, nucleosynthetic isotope effects of this magnitude are unlikely for Tl, as they are also not observed for other elements of similar atomic mass, such as Hf, Os, and Pt (Kruijer et al., 2013; Sprung et al., 2010; Walker, 2012; Yokoyama et al., 2007). Thallium isotope data acquired for metal-silicate and sulfide-silicate partitioning experiments furthermore demonstrate that Tl

391 isotope fractionation during metal or sulfide segregation is either very small or absent (Wood et
392 al., 2008).

393 As a consequence, Andreasen et al. (2012) suggested an alternative interpretation of the
394 carbonaceous chondrite and magmatic iron meteorites isochrons. By discarding the results of all
395 four carbonaceous chondrites, which featured significant quantities of terrestrial Pb
396 contamination (at about 10 to 80% of total measured Pb), a revised carbonaceous chondrite
397 isochron with a significantly steeper but less well-defined slope was obtained. This revised
398 calculation yields $^{205}Pb/^{204}Pb_{SS,0} = (2\pm1)x10^{-3}$ and $\varepsilon^{205}Tl_{SS,0} = -13.6$. Using this initial solar
399 system $^{205}Pb_{SS,0}$ abundance, the IIAB and IIIAB isochrons now provide ages of 15 +20/-12 Ma
400 and 14 +32/-15 Ma, respectively. It is unknown, however, whether these ages date core
401 crystallization or are linked to the breakup of the meteorite parent bodies. Likewise the IAB
402 isochron now gives a younger age of 69 +16/-10 Ma after the carbonaceous chondrites, and this
403 may indicate that the Pb-Tl decay system dates the same impact event(s) that are recorded in the
404 ~4.5 Ga Ar-Ar ages of IAB silicate inclusions (Vogel and Renne, 2008). Notably, the revised
405 initial solar system ^{205}Pb abundance of $^{205}Pb/^{204}Pb_{SS,0} = (2\pm1)x10^{-3}$ is somewhat higher than the
406 upper estimate that was obtained in models of s-process nucleosynthesis by Wasserburg et al
407 (2006). Whether this discrepancy reflects uncertainties in the analytical data, the stellar models,
408 or in the estimates of recent s-process contributions to the solar nebula, remains unclear at
409 present.

410

411 **3.3. Limitations of the ^{205}Pb–^{205}Tl chronometer**

412 In principle, the ^{205}Pb–^{205}Tl decay system offers many promising applications but translation
413 of this potential has been hindered by a number of factors. (i) Due to the low abundances of Tl in

many meteorites, large samples of typically more than 1 g but with >10 g not uncommon, have been used for precise Tl isotope measurements. These requirements make analyses challenging and measurements for highly volatile depleted meteorites (e.g., IVA/B irons and many achondrites) have not been attempted to date. (ii) As a result of the highly labile nature of Tl, isochronous behavior is easily disturbed or fully reset. In addition, remobilization of Tl can be associated with stable isotope fractionation, which hampers unambiguous interpretations. (iii) The pervasive contamination of many meteorites with terrestrial Pb renders the determination of robust primitive $^{204}Pb/^{203}Tl$ ratios (as required for Pb-Tl isochron calculations) and initial $^{205}Pb/^{204}Pb$ values very difficult. Analyses of such contaminated meteorites requires that anthropogenic Pb is removed from samples by thorough cleaning and/or corrections for the effects of contamination must be attempted, based on Pb isotope data. Such corrections, however, can be subject to large uncertainties whilst aggressive cleaning of samples by leaching and/or partial dissolution (as is commonly applied prior to analyses of radiogenic Pb isotope compositions) can lead to partial Tl loss that may be associated with isotope fractionation.

4. THALLIUM ISOTOPE COMPOSITON OF THE SOLID EARTH

4.1. The primitive mantle

The concentration of Tl in the primitive mantle has been estimated as 0.0035 μg/g (McDonough and Sun, 1995) and for the depleted mantle as 0.00038 μg/g (Salters and Stracke, 2004). The challenge associated with evaluating the Tl concentration and isotope composition of the mantle is largely twofold. First, thallium concentrations are vanishingly low, thus grams of material are required to obtain precise concentration and/or isotope measurements by bulk rock dissolution approaches. Minute inclusions of secondary alteration products such as clays that

437 easily incorporate Tl are much more problematic with very large sample sizes, and any such
438 material can drastically affect the determination of both Tl concentration and isotope
439 composition. Second, even though the required sample sizes are large, there is still worrying
440 potential for 'nugget' effects. For example, Nielsen et al. (2014) have shown by laser-ablation
441 inductively coupled plasma mass spectrometry (LA-ICPMS) that the only phase housing
442 significant Tl in the Lherz peridotite massif, France, are interstitial sulfides, which yielded
443 variable Tl concentrations from 0.023 to 0.430 μg/g. All other investigated mineral phases
444 (olivine, orthopyroxene, clinopyroxene and spinel) had Tl concentrations below detection limit,
445 restricting the Tl concentration in the vast majority of mantle minerals to < 0.001 μg/g (Nielsen
446 et al., 2014). An experimental study by Kiseeva and Wood (2013) further documents Tl partition
447 coefficients between sulfide liquid and a silicate melt with MORB composition of $D_{Tl}^{sulf/sil}$ = 4.1
448 to 18.8, reinforcing the notion that sulfides are the main host for Tl, at least in the upper mantle.
449 To date, only a single measurement of a mantle xenolith has been published (Nielsen et al.,
450 2015). The sample, a harzburgite from the Eifel volcanic field in Germany, revealed an isotope
451 composition of $\varepsilon^{205}Tl$ = -2.0±0.8 and concentration of 1.05 ng/g. The concentration is, thus,
452 slightly higher than what would be expected based on published estimates of Tl in the depleted
453 mantle (Salters and Stracke, 2004), but given the potential for nugget effects it is unclear if the
454 concentration is necessarily representative of the upper mantle.
455 Due to the problems associated with direct measurements, Nielsen et al. (2006b) used five
456 fresh, glassy MORBs from different global ocean basins to estimate the Tl isotope composition
457 of the mantle. The homogeneity of the results ($\varepsilon^{205}Tl_{MORB}$ = -2±1; Fig 1) strongly indicates that
458 no large-scale geographic Tl isotopic differences exist in the present day upper mantle
459 uncontaminated by crustal components. Given that these lavas are not derived from identical

460 degrees of melting, the restricted range in ε^{205}Tl strongly suggests that partial melting of the
461 mantle does not fractionate Tl isotopes to an analytically resolvable level. This inference is
462 further supported by the identical Tl isotope composition of these MORBs and the published
463 harzburgite sample (Nielsen et al., 2015) and not unexpected, given the heavy atomic masses of
464 Tl isotopes. However, since stable isotope fractionation has been observed for some lighter
465 elements during mantle melting (e.g., Fe isotopes; (Craddock et al., 2013; Williams et al., 2004)),
466 further Tl isotope analyses of MORB and peridotites are desirable to validate this assumption.
467
468 **4.2. The continental crust**
469 As discussed, Tl generally follows the alkali metals K, Rb and Cs during melting and
470 fractional crystallization (Heinrichs et al., 1980; Shaw, 1952) resulting in much higher Tl
471 concentrations in the continental crust (~0.5 μg/g) versus the primitive mantle (~0.0035 μg/g)
472 (Heinrichs et al., 1980; McDonough and Sun, 1995; Rudnick and Gao, 2003; Shaw, 1952;
473 Wedepohl, 1995).
474 Although the chemical affinity with K, Rb, and Cs suggests lithophile behavior, thallium
475 has been considered both a chalcophile and lithophile element. McGoldrick et al. (1979)
476 suggested that Tl displays chalcophile behavior and follows sulfur in sulfur-saturated magmas. In
477 contrast, a study of sulfur-rich ore deposits (Baker et al., 2010a) found that Tl retained strong
478 lithophile behavior in this setting. Noll et al. (1996) assumed that Tl behaved as a chalcophile
479 element and used chalcophile/lithophile element ratios in subduction-related lavas to determine
480 relative fluid mobility of trace elements. They suggested that Tl has a similar bulk partition
481 coefficient to La. However, Tl showed no significant correlation with 'fluid-mobile' and
482 chalcophile elements such as As, Sb and Pb, again casting doubt on its chalcophile affinity in

483 evolving magmatic systems. A study of lavas from the Mariana arc also suggests lithophile,
484 fluid-immobile behavior, demonstrated by strong co-variation of Tl with La, rather than Ba
485 (Prytulak et al., 2013). Thus the elemental behavior of Tl during magmatic processes and the
486 specific controls on its concentration in the continental crust remain ambiguous. This ambiguity
487 is underlined by the strong affinity Tl has for sulfides formed in aqueous low temperature
488 hydrothermal systems (Xiong, 2007), mantle sulfides and early diagenetic pyrite (Nielsen et al.,
489 2011; Nielsen et al., 2014).

490 The lack of resolvable isotope differences in global MORB suggests that negligible Tl
491 isotope fractionation occurs during moderate degrees of partial melting (15-20%). Given the
492 evolved bulk composition of the continental crust, it is necessary to consider the impact of
493 further igneous processes on Tl stable isotope fractionation. Though stable isotope fractionation
494 has been documented during igneous processes for relatively heavy elements such as iron (e.g.
495 Williams et al., 2004; Williams et al., 2009), the small relative mass difference between the
496 isotopes of Tl in combination with little or no redox chemistry for Tl in igneous systems, favor
497 negligible Tl isotope fractionation during magmatic processes. Several studies found that the
498 isotope composition of the average upper continental crust, represented by loess, is
499 indistinguishable from MORB, with both exhibiting a value of $\varepsilon^{205}Tl = -2.0 \pm 0.5$ (Nielsen et al.,
500 2007; Nielsen et al., 2006b; Nielsen et al., 2005b; Nielsen et al., 2006c). The uniform isotope
501 composition of the continental crust is further supported by data obtained for an ultrapotassic
502 dike from the Tibetan Plateau ($\varepsilon^{205}Tl = -2.3 \pm 0.5$), which represents a melt originating from the
503 sub-continental lithospheric mantle (Williams et al., 2001). Finally, Nielsen et al., (2016)
504 recently determined $\varepsilon^{205}Tl$ in a suite of co-genetic basalts through andesites from a single
505 volcano on Atka Island in the Aleutian arc. Thallium concentrations display strong positive co-

506 variation with K_2O wt%, as expected for an incompatible element during fractional
507 crystallization. Although the lavas range in $\varepsilon^{205}Tl$ from -2.3 to +0.7, the isotope values do not
508 co-vary with Tl concentration and the variability is instead attributed to subduction zone inputs.
509 Hence, on balance, there is little evidence to suggest that melting or fractional crystallization
510 imparts analytically resolvable Tl isotope fractionation and therefore the bulk continental crust
511 can be characterized by $\varepsilon^{205}Tl_{CONTCRUST} = -2 \pm 1$ (Fig. 1).
512
513 **5. THALLIUM ISOTOPE COMPOSITION OF SURFACE RESERVOIRS**
514 **5.1. Volcanic degassing**
515 Due to its low boiling point (Table 1), Tl is significantly enriched in volcanic gasses and
516 particles compared with the geochemically analogous alkali metals (Baker et al., 2009; Gauthier
517 and Le Cloarec, 1998; Hinkley et al., 1994; Patterson and Settle, 1987). Consequently, volcanic
518 plumes provide a large Tl flux from igneous to surface environments on Earth, with an estimated
519 flux to the oceans of 370 Mg/a (Baker et al., 2009; Rehkämper and Nielsen, 2004). The behavior
520 of Tl isotopes during degassing in volcanic systems was investigated by Baker et al. (2009), who
521 identified significant isotope variations. The most likely form of isotope fractionation to occur
522 during degassing is kinetic isotope fractionation, where the light isotope is enriched in the gas
523 phase during evaporation. The extent of kinetic isotope fractionation between two phases is
524 determined by the relative magnitude of the atomic or molecular velocities, where $\alpha = (m_1/m_2)^{\beta}$
525 and β varies from 0.5 (in the case of a vacuum) down to values approaching 0 (Tsuchiyama et
526 al., 1994). Hence, even though the relative mass difference between the two Tl isotopes is small,
527 the maximum kinetic $\alpha_{liq\text{-}vap}$ is 1.0049, equivalent to a fractionation factor of 49 ε-units. An
528 isotopic difference of this magnitude exceeds the stable Tl isotope variability currently known

for Earth and should hence be readily detectable. However, contrary to the expectation of a gas phase enriched in light isotopes, Baker et al. (2009) found no systematic enrichment of either ^{203}Tl or ^{205}Tl in volcanic emanations compared with average igneous rocks. Despite large isotopic differences between individual samples, the isotope compositions of 34 samples of gas condensates and particles from six separate volcanoes showed an average of ε^{205}Tl = -1.7 ± 2.0. This value is indistinguishable from average igneous rocks (Nielsen et al., 2007; Nielsen et al., 2006b; Nielsen et al., 2005b; Nielsen et al., 2006c; Nielsen et al., 2016; Prytulak et al., 2013) and suggests that degassing as a whole does not significantly alter that Tl isotope composition of degassed lavas. The Tl isotope variation of volcanic emanations was interpreted to reflect the complex evaporation as well as condensation processes that occur in volcanic edifices (Baker et al., 2009), and which eventually produce no net isotope fractionation between Tl in the magma and the Tl transported into the atmosphere and surface environments on Earth.

5.2. Weathering and riverine transport of Tl

Stable isotope fractionation during weathering is often monitored via measurements of isotope ratios in the dissolved and particulate phases in rivers. For example, elements like lithium and molybdenum have been shown to display significant isotopic variation between different rivers and rocks of the continental crust (e.g. Archer and Vance, 2008; Huh et al., 1998; Pogge von Strandmann et al., 2010). Numerous kinetic and equilibrium processes can potentially affect the stable isotope budgets of rivers, and as such it is difficult to predict isotope fractionation during weathering. In general, Tl is soluble in aqueous solution and should be readily mobilized during weathering. However, the tendency for Tl to partition into potassium rich minerals and manganese oxides (Heinrichs et al., 1980) suggests that the transport of Tl into the ocean may be

552 less efficient. Nielsen et al. (2005b) measured the Tl isotope compositions of dissolved and
553 particulate components for a number of major and minor rivers and found that these generally
554 display values similar to those observed for continental crust. The average value for dissolved
555 riverine Tl is $\varepsilon^{205}Tl = -2.5 \pm 1.0$ (Nielsen et al., 2005b), with particulate matter ($\varepsilon^{205}Tl = -2.0 \pm$
556 0.5) being indistinguishable from the dissolved phase (Table 3). Although there are clearly
557 resolvable differences in riverine Tl isotope compositions that were inferred to be related to
558 variations in catchment litholigies, the majority of rivers including the worlds largest, the
559 Amazon, display $\varepsilon^{205}Tl$ values similar to average continental crust. These data strongly imply
560 that there is little or no Tl isotope fractionation associated with continental weathering processes.
561 Natural unpolluted Tl abundances in rivers are generally very low and vary between 1 and
562 10 pg/g (Cheam, 2001; Nielsen et al., 2005b). An estimated global average dissolved riverine
563 concentration of 6±4 pg/g (or 30±20 pmol/l) results in a flux to the oceans of 230 Mg/yr. In the
564 study of Nielsen et al. (2005b) three rivers exhibited Tl isotope compositions significantly lighter
565 (at $\varepsilon^{205}Tl = -6$ to -4) than average continental crust (Table 3). The lower $\varepsilon^{205}Tl$ values were
566 interpreted to reflect weathering of marine carbonates that are a main constituent of the drainage
567 areas for these rivers. Relatively light Tl isotope compositions are expected for such carbonates
568 based on analyses of modern seawater, which is characterized by $\varepsilon^{205}Tl = -6.0 \pm 0.3$ (Nielsen et
569 al., 2004; Nielsen et al., 2006c; Owens et al., 2016; Rehkämper et al., 2002). However, marine
570 carbonates including carbonate oozes (Rehkämper et al., 2004), corals (Rehkämper, unpublished
571 data) and foraminifera (Nielsen, unpublished data) exhibit very low Tl concentrations. This
572 implies that weathering of marine carbonates will only have a strong impact on the Tl inventories
573 of rivers that predominantly drain such lithologies and will not strongly affect the total global
574 budget of Tl transported by rivers to the oceans.

575

576 **5.3. Anthropogenic mobilization of Tl**

577 Similar to its periodic table neighbors Hg, Cd, and Pb, Tl is also readily volatilized by high-
578 temperature processes, such as combustion. As a consequence, the most important global source
579 of anthropogenic Tl are atmospheric emissions from processes such as pyrite roasting, cement
580 production and coal burning, and associated solid wastes. In addition, Tl release with wastewater
581 from ore processing plants can have a significant impact on terrestrial aquatic system (Nriagu,
582 1998; Peter and Viraraghavan, 2005).

583 Like its elemental neighbors, Tl also has a high acute and chronic toxicity to mammals,
584 including humans. Due to the low concentrations of Tl in most natural and manufactured
585 materials, and its limited use in consumer products or industrial processes, anthropogenic Tl
586 emissions to the environment are fortunately generally low. They only represent a significant
587 health hazard in the vicinity of significant emission sources, particularly when aided by
588 bioaccumulation in the food chain (Nriagu, 1998; Peter and Viraraghavan, 2005). Such a case of
589 chronic Tl poisoning was reported for the inhabitants of a rural village in the Lanmuchang area
590 of Guizhou Province, China. The village is situated in close proximity to a massive vein of Tl
591 mineralization that has a protracted history of artisanal mining (Xiao et al., 2003; Xiao et al.,
592 2004). The health effects seen in the villagers (including muscle and joint pain, hair loss, and
593 disturbance or even loss of vision) were traced to the consumption of local crops (particularly
594 highly Tl-enriched green cabbage), which are grown on soils with elevated Tl concentrations
595 from past mining activities (Xiao et al., 2004; Xiao et al., 2007).

596 The isotopic signature of Pb, which is highly variable due to radiogenic ingrowth from the
597 decay of U and Th isotopes, has long been used to fingerprint anthropogenic Pb emissions to the

598 environment, particularly from the use of leaded gasoline (Alleman et al., 1999; Rosman et al.,
599 1994; Settle and Patterson, 1982). Following the advent and more widespread application of
600 MC-ICP-MS, a number of studies demonstrated that similar fingerprinting is also feasible for Hg
601 and Cd emissions, based on analyses of the stable isotope compositions of these elements
602 (Rehkämper et al., 2012; Ridley and Stetson, 2006). More recently, an investigation by Kersten
603 et al. (2014) demonstrated, for the first time, that Tl stable isotope compositions can also be used
604 as a tracer of anthropogenic Tl emissions to the environment.

605 In the study of Kersten et al. (2014), Tl isotope data were used to link the high Tl contents
606 of agricultural soils to past emissions of cement kiln dust (CKD) from a nearby cement plant in
607 Lengerich, northwest Germany. In detail, it was shown that the soils were contaminated by Tl
608 emissions that occurred in the 1970's, when the cement plant utilized pyrite-roasting waste with
609 high Tl contents as a cost-effective, S-rich additive during cement production, a process that
610 involves combustion processes at temperatures of more than 1000º C. To arrive at this
611 conclusion, contaminated soil samples from three vertical profiles with up to 1 m depth were
612 analyzed for both Tl concentrations and isotope compositions. When viewed in a diagram of
613 ε^{205}Tl versus inverse Tl concentration (1/[Tl]), the soil data are strongly indicative of a binary
614 mixing relationship (Fig. 6). The mixing endmembers were inferred to be the geogenic
615 background, as defined by isotopically light soils with $\varepsilon^{205}Tl \approx -4$ at depth, and the Tl emissions,
616 represented by Tl-enriched topsoils with a distinctly heavier isotopic signature of $\varepsilon^{205}Tl \approx 0$. This
617 conclusion is further corroborated by Tl isotope compositions of $\varepsilon^{205}Tl \approx \pm 0$ that were obtained
618 for (i) a CKD sample taken at the time of the inferred Tl emissions and (ii) a pyrite, which was
619 sourced from the same Weggen deposit in Germany as the pyrite roasting waste that was added
620 to the cement raw mix prior to combustion in the kiln (Fig. 6).

621 Additional analyses were carried out by Kersten et al. (2014) for soil and crop samples from
622 the Lanmuchang area (Guizhou Province) in China. These measurements revealed significant
623 isotope fractionation between soils, with a high natural Tl background characterized by $\varepsilon^{205}Tl \approx$
624 +0.4, and locally grown cabbage, which displayed $\varepsilon^{205}Tl$ values of between –2.5 and –5.4. This
625 demonstrates that biological isotope fractionation and subsequent remineralization of Tl from
626 organic material cannot be responsible for the heavier Tl isotope signatures that were found in
627 the Lengerich topsoil. Rather, the high Tl contents and associated heavier isotope signatures seen
628 in the vicinity of the Lengerich cement plant are most reasonably explained by Tl emissions that
629 were released during cement production (Kersten et al., 2014).
630
631 **5.4. The isotope composition of seawater**
632 In the oceans, Tl is a conservative, low-level trace element with an average dissolved
633 concentration of 13±1 pg/g (64±5 pmol/l) (Flegal and Patterson, 1985; Nielsen et al., 2006c;
634 Rehkämper and Nielsen, 2004; Schedlbauer and Heumann, 2000). The seawater average is
635 thereby slightly higher than the dissolved Tl abundances of most rivers (see section 5.2). Based
636 on a thorough review of the marine input and output fluxes of Tl, Rehkämper and Nielsen (2004)
637 concluded that the oceans are currently at steady state and that Tl has a residence time of ~21 ka,
638 which is consistent with a number of previous studies (Flegal and Patterson, 1985; Flegal et al.,
639 1989). With an inferred marine residence time that is more than an order of magnitude longer
640 than the ocean mixing time and a conservative distribution, Tl should exhibit an invariant isotope
641 composition in seawater. Analyses of Arctic, Atlantic and Pacific seawater confirm this
642 prediction (Nielsen et al., 2004; Nielsen et al., 2006c; Rehkämper et al., 2002). In particular, a
643 recent data set for about 50 samples covering the GEOTRACES GA10 transect in the Atlantic

644 across 40°S shows no Tl isotope variation, with an overall average of $\varepsilon^{205}Tl = -6.0\pm0.3$ (Owens
645 et al., 2016). The invariance of the GA10 data is remarkable because a number of different water
646 masses are present in this transect (Antarctic Bottom Water, North Atlantic Deep Water,
647 Antarctic Intermediate Water) that are sourced from very disparate regions of the ocean.
648 Therefore, these analyses confirm that the open ocean is homogenous with respect to Tl isotopes
649 within current measurement uncertainties.

650 It may be somewhat surprising that the oceans are significantly enriched in ^{203}Tl compared
651 to the continental crust and the mantle (see Section 4) with an average value of $\varepsilon^{205}Tl = -6.0\pm0.3$
652 (Nielsen et al., 2004; Nielsen et al., 2006c; Owens et al., 2016; Rehkämper et al., 2002). Hence,
653 it is required either that the marine sources of Tl are isotopically light compared to the
654 continental crust and mantle or that the outputs are fractionated towards heavy isotope
655 compositions relative to seawater. Rehkämper and Nielsen (2004) showed that the most
656 significant marine inputs for Tl are from rivers, high-temperature hydrothermal fluids, mineral
657 aerosols, volcanic emanations and sediment pore water fluxes at continental margins. In contrast,
658 there are only two important marine Tl sinks, namely Tl adsorption by the authigenic phases of
659 pelagic clays and uptake of Tl during low-temperature alteration of oceanic crust. The relative
660 magnitudes and isotope compositions of these fluxes are summarized in Table 4. In the following
661 sections, we outline the main observations that follow from an assessment of these fluxes.
662

6. THE MARINE MASS BALANCE OF THALLIUM ISOTOPES

6.1. Thallium isotopes in marine input fluxes

As riverine and volcanic input fluxes were already discussed in previous sections, we will here focus on high-temperature hydrothermal fluids, mineral aerosols and sediment pore water fluxes from continental margins.

6.1.1. High temperature hydrothermal fluids

In hydrothermal systems where temperatures exceed ~150°C it has been shown that Tl behaves much like the alkali metals Rb and K (Metz and Trefry, 2000), and is leached from the oceanic crust by circulating fluids. The efficiency of this leaching process is roughly 90%, as shown by Ce/Tl ratios in the sheeted dike complex of ODP Hole 504B that are ~10 times higher than in pristine MORB (Fig. 7). This results in end-member high temperature hydrothermal fluids that exhibit Tl concentrations almost 500 times higher compared to ambient seawater (Metz and Trefry, 2000; Nielsen et al., 2006c). We can estimate the flux of Tl into the oceans (M_{Tl}) from high-T hydrothermal fluids by combining the average Tl concentration of MORB with the flux of ocean crust leached by high-T fluids, assuming 90% leaching efficiency:

$$M_{Tl} = F_{oc\ leach} \times [Tl]_{oc} \times f_{Tl\ leach} \quad (2)$$

Here, $F_{oc\ leach}$ is the annual production rate of ocean crust that is leached by high-T fluids, $[Tl]_{oc}$ is the Tl content of the crust prior to leaching, and $f_{Tl\ leach}$ is the fraction of Tl leached from the rocks during alteration. The annual production rate of ocean crust leached by high-T fluids is comprised of ~$1.24\pm0.16\times10^{16}$ g/a of MORB crust and ~$0.76\pm0.10\times10^{16}$ g/a of cumulate lower ocean crust with Tl concentration estimated at 25% of the fresh MORB value (Mottl, 2003; Nielsen et al., 2006c).

686 It was previously thought that Tl partitioned similarly to Cs during mantle melting (Jochum
687 and Verma, 1996; Nielsen et al., 2006b), which, based on an assumed Cs/Tl ≈ 6, yielded a Tl
688 content of ~3 ng/g for fresh MORB. However, more recent data has shown that Tl is much more
689 compatible during mantle melting because it partitions into sulfides (Kiseeva and Wood, 2013;
690 Nielsen et al., 2014). Although there is a relatively large database for Tl concentrations in fresh
691 MORB (Jenner and O'Neill, 2012; Nielsen et al., 2014), the global average Tl concentration for
692 MORB is best determined by combining the constant Ce/Tl = 1110±330 for MORB with >6%
693 MgO (Nielsen et al., 2014) with the global weighted average Ce concentration for MORB of
694 14.86±1.26 μg/g (Gale et al., 2013), because Ce data for MORB have a complete global
695 coverage. This combination yields a global average Tl concentration in MORB of 13.4±4.2 ng/g,
696 which is similar to the value obtained by averaging all available Tl data for MORB (12±8ng/g)
697 (Jenner and O'Neill, 2012; Nielsen et al., 2014). Inserting the three parameters into equation (2)
698 produces an annual Tl flux into the ocean from high-T hydrothermal fluids of 170±60 Mg/yr.
699 Due to the relatively high temperatures involved (300-400°C), isotope fractionation is not
700 expected to be significant. This inference was confirmed by Nielsen et al. (2006c), who
701 determined the Tl isotope composition of hydrothermal fluids from the East Pacific Rise and
702 Juan de Fuca Ridge. All samples had Tl isotope compositions identical to that of average
703 MORB, thus supporting the interpretation that extraction of Tl from the oceanic crust is not
704 associated with isotope fractionation. The chemical and isotopic behavior inferred for Tl from
705 hydrothermal fluids is furthermore in accord with the results of a study of oceanic crust altered
706 by high temperature hydrothermal fluids from ODP Hole 504B. The latter work revealed Tl
707 concentrations for basalts and dikes that were much lower than expected for depleted ocean crust
708 whilst the Tl isotope compositions were identical to average MORB (Nielsen et al., 2006c).

709

710 *6.1.2. Mineral aerosols*

711 There are no direct investigations of Tl abundances or isotope compositions for mineral
712 aerosols deposited in the oceans. Based on studies of windborne loess sediments deposited on
713 land, Nielsen et al. (2005b) concluded that the average abundance of Tl in dust deposited in the
714 oceans is about 490±130 ng/g. The main uncertainty in determining the Tl flux to the oceans is
715 from estimating the fraction of Tl that is released from the dust into seawater, following
716 deposition and partial dissolution. By comparison with a number of other elements, Rehkämper
717 and Nielsen (2004) concluded that about 5-30% of the Tl transported in aerosol particles would
718 dissolve in seawater, resulting in an annual Tl flux of 10 – 150 Mg/yr.

719 It may be reasonable to assume that the bulk Tl isotope composition of the material
720 transported to the ocean is identical to loess, and thereby also the continental crust, with $\varepsilon^{205}Tl$ =
721 -2 (Nielsen et al., 2005b). However, it is unknown whether dust dissolution is associated with
722 isotope fractionation. Schauble (2007) has shown that significant equilibrium Tl isotope
723 fractionations will be produced primarily by chemical reactions that involve both valence states,
724 Tl^{+} and Tl^{3+}. Based on the strongly correlated behavior of Tl, Rb, Cs and K in the continental
725 crust, univalent Tl should be dominant in mineral aerosols. Thermodynamic calculations of the
726 valence state of Tl in seawater also predict that all Tl is univalent in this reservoir (Nielsen et al.,
727 2009a). In addition, continental weathering processes, which are ultimately controlled by
728 aqueous dissolution of silicates and are therefore in some ways analogous to the partial
729 dissolution of dust in seawater, induce no detectable Tl isotope fractionations (Nielsen et al.,
730 2005b). Hence, we infer that isotope fractionation is unlikely to be significant during the
731 dissolution of mineral aerosols in seawater.

732

733 *6.1.3. Benthic fluxes from continental margins*

734 It has long been known that pore waters, which seep into the oceans from reduced
735 continental margin sediments, are rich in Mn (Elderfield, 1976; Sawlan and Murray, 1983). As
736 Tl has a high affinity to Mn oxides (Koschinsky and Hein, 2003) and is more soluble in seawater
737 than Mn, it has been inferred that such pore waters may be an important source of dissolved
738 marine Tl (Rehkämper and Nielsen, 2004). However, there are currently no direct data available
739 for sediment pore fluids to constrain either the average Tl concentration or isotope composition
740 of these benthic fluxes. An estimate was therefore derived indirectly, based on (1) Tl/Mn ratios
741 observed in ferromanganese nodules that were known to have precipitated from pore waters
742 (Rehkämper et al., 2002), combined with (2) estimates for benthic Mn fluxes (Heggie et al.,
743 1987; Johnson et al., 1992; Sawlan and Murray, 1983). Taken together, these data yield a Tl flux
744 of 5 – 390 Mg/a, and a best estimate of 170 Mg/a (Rehkämper and Nielsen, 2004), which
745 constitutes a substantial fraction of the total Tl flux to the oceans (Table 4).

746 We can use two distinct approaches to estimate the average Tl isotope composition of pore
747 waters. The first utilizes published Tl isotope data for the various components that may supply
748 pore waters. The second relies on the Tl isotope compositions of sediments, which contain a
749 component that was precipitated from pore waters. The application of these approaches is
750 summarized below.

751 There are three principle components, from which Tl could be mobilized and incorporated
752 into sedimentary pore waters. (1) Labile Tl associated with riverine particles (Nielsen et al.,
753 2005b). (2) Thallium adsorbed onto clay minerals from seawater (Matthews and Riley, 1970). (3)
754 Thallium bound to authigenic Mn-oxides that precipitated from seawater as part of pelagic red

755 clays (Rehkämper et al., 2004). All three will be present in continental margin sediments in
756 various proportions depending on sedimentation rate and proximity to estuaries, where high
757 sedimentation rates will tend to dilute the Mn-oxides, as authigenic precipitation should remain
758 fairly constant. Hence, assuming that there is no isotope fractionation associated with the release
759 of Tl into pore waters, the isotope composition of each component provides bounds on the
760 composition of pore waters.

761 The labile components in riverine particles have been shown to be isotopically similar to the
762 continental crust and river waters and are thus characterized by $\varepsilon^{205}Tl = -2$ (Nielsen et al.,
763 2005b). Matthews and Riley (1970) showed that Tl is readily adsorbed onto some clay minerals
764 (in particular illite) where most Tl is exchanged with K. Because of the required charge balance
765 for adsorption reactions, Tl adsorption onto clays is unlikely to be associated with any Tl
766 reduction/oxidation and should thereby exhibit only minimal or no isotope fractionation
767 (Schauble, 2007). Since Tl adsorption by clay minerals will take place primarily within the
768 marine environment, this component should inherit the Tl isotope composition from seawater of
769 $\varepsilon^{205}Tl = -6.0$.

770 Thallium that is precipitated with Mn oxides onto sedimentary particles has been shown to
771 have a significantly heavier isotope composition than the seawater from which the mineral forms
772 (Rehkämper et al., 2004; Rehkämper et al., 2002). The origin of this isotope fractionation is
773 discussed in section 5 below. Theoretically, the pure MnO_2 mineral to which Tl is bound should
774 have approximately the same isotope composition as the surfaces of Fe-Mn crusts, which display
775 $\varepsilon^{205}Tl \approx +13$ (Fig. 8). However, leaching experiments conducted on shelf sediments with HCl
776 and hydroxylamine hydrochloride indicate that the labile Tl on sediment particles features
777 somewhat lower $\varepsilon^{205}Tl$ values of between +3 to +7 (Nielsen et al., 2005b; Rehkämper et al.,

778 2004). These lower values could reflect contributions from components other than Fe-Mn oxides,
779 particularly Tl incorporated into carbonates or adsorbed to clay minerals, with both presumably
780 characterized by negative ε^{205}Tl. Nevertheless, it appears reasonable to infer that the Tl
781 associated with marine authigenic Mn in continental margin sediments exhibits ε^{205}Tl ≈ +4 to
782 +10.

783 In summary, the isotopic data available for these three components indicate that pore waters
784 from continental margin sediments are likely to feature ε^{205}Tl values of about -4 to +6. This
785 range can be compared with the compositions of two different sedimentary archives that form
786 from pore waters. These are diagenetic ferromanganese nodules (which are inferred to originate
787 primarily from pore waters) and early diagenetic pyrite. Rehkämper et al. (2002) analyzed two
788 Mn nodules from the Baltic Sea and these exhibited ε^{205}Tl = -0.2 and -5.2. Nielsen et al. (2011)
789 measured Tl isotopes in pyrites younger than 10 Ma from continental shelf sediments in the
790 Northeast Pacific and the Caribbean and found ε^{205}Tl values of between -1 to +2. Importantly,
791 both ferromanganese nodules and pyrites have Tl isotope compositions that are in accord with
792 the range of values inferred for pore waters based on their constituent components. Taken
793 together (and assuming that there is negligible isotope fractionation between pyrite/Fe-Mn
794 nodules and pore waters) these constraints suggests that benthic fluxes from continental shelf
795 sediments are characterized by ε^{205}Tl ~ -3 to +3, with a best estimate of ε^{205}Tl ≈ 0.
796
797

6.2. Thallium isotope compositions of marine output fluxes

6.2.1. Thallium adsorption by the authigenic phases of pelagic clays

There is a significant enrichment of Tl in pelagic clays compared with continental shelf sediments (Heinrichs et al., 1980; Matthews and Riley, 1970; Rehkämper et al., 2004). This enrichment is caused by the adsorption of Tl onto hydrogenetic Fe-Mn oxy-hydroxides and clay minerals (Heinrichs et al., 1980; Matthews and Riley, 1970; McGoldrick et al., 1979). Two independent methods of calculating the Tl flux associated with these authigenic fluxes agree very well and indicate an annual flux of 200-410 Mg/a, with a best estimate of 270 Mg/a (Rehkämper and Nielsen, 2004). If the smaller flux of Tl incorporated into pure Fe-Mn deposits of ~40 Mg/a (Rehkämper and Nielsen, 2004) is also considered, this yields a total marine authigenic Tl flux of 310 Mg/a (Table 4). As discussed in section 6.1.3, the isotope composition of the Tl associated with authigenic phases is best approximated as a mixture of Tl bound to Mn oxides that probably display $\varepsilon^{205}Tl \approx +13$ and Tl adsorbed onto clay minerals, which likely exhibit the composition of seawater ($\varepsilon^{205}Tl \approx -6$). Due to the strong enrichment of Mn in pelagic clays, it can be assumed that the majority of authigenic Tl in such sediments originates from Mn oxides and thus may have an isotope composition more akin to Fe-Mn crusts. We can attempt to quantify this effect by performing an isotope mass balance calculation for the modern (core-top) pelagic clays reported in Rehkämper et al. (2004). The bulk isotope composition of these samples is $\varepsilon^{205}Tl =$ +3 to +5. About 50% of the Tl in pelagic clays is thought to be of detrital origin (Rehkämper et al., 2004), which is characterized by $\varepsilon^{205}Tl = -2$ (Nielsen et al., 2005b). In order to account for the reported bulk isotope compositions, the authigenic component would thus have to display $\varepsilon^{205}Tl \sim +8$ to +12, and this implies that the authigenic Tl of pelagic clays features an isotope composition that is slightly lighter than pure Fe-Mn deposits. Based on the above considerations

821 we can calculate that ~75-95% of the authigenic Tl in pelagic clays originates from Mn-oxides,
822 whilst the remainder is bound to clay minerals.
823
824 *6.2.2. Thallium uptake during low temperature hydrothermal alteration*
825 It is well known that alteration minerals produced by interaction between cold (<100°C)
826 seawater and MORB are highly enriched in Tl compared to pristine oceanic crust (Alt, 1995;
827 Jochum and Verma, 1996; McGoldrick et al., 1979), and this leads to a strong Tl enrichment in
828 the upper 500-600m of the oceanic crust (Fig. 7a). It is unclear, however, which alteration
829 mineral(s) are primarily responsible for accommodating the additional Tl. Palagonitization
830 causes substantial deposition of Tl, which has been attributed to partitioning into smectites and
831 other alkali-rich clay minerals (Jochum and Verma, 1996; McGoldrick et al., 1979). In contrast,
832 altered assemblages from IODP Hole U1301B appear to show correlations between bulk Tl and
833 S concentrations, which led to the interpretation that the main carrier phase for Tl during
834 hydrothermal alteration is pyrite (Coggon et al., 2014). Lastly, composites from several depth
835 intervals in Jurassic oceanic crust from ODP Hole 801C showed no clear Tl enrichment and
836 limited isotope fractionation compared with $\varepsilon^{205}Tl_{MORB}$ = -2±1 (Fig. 7). The uncertainties in
837 depositional mechanism, combined with the highly heterogeneous distribution of Tl in low-T
838 altered oceanic crust (Coggon et al., 2014; Nielsen et al., 2006c; Prytulak et al., 2013; Teagle et
839 al., 1996), complicate efforts to estimate the average Tl concentration of low-T altered oceanic
840 crust and determine the annual flux of Tl into this reservoir. Following a conservative approach it
841 was proposed that, on average, the upper 600m of oceanic crust contains 200±150 ng/g of Tl
842 (Nielsen et al., 2006c), although the number is based mostly on inferred values rather than actual
843 data. The Tl concentration estimate is equivalent to an element flux of 225-1985 Mg/a, with a

844 best estimate of ~1000 Mg/yr. The preferred estimate, however, is similar to the combined flux
845 of all marine Tl inputs (Table 4).

846 Given the uncertainties, it may thus be more reasonable to apply a mass balance approach
847 (which assumes that marine Tl is at steady state) to estimate the Tl flux into low-T altered ocean
848 crust. With a total input flux of 990 Mg/a (Table 4) and an authigenic output flux of 310 Mg/a,
849 the marine Tl budget can be balanced with a low-T alteration output of 680 Mg/a, which is well
850 within the range of values estimated based on Tl concentration data available for low-T altered
851 ocean crust (Table 4). The reconstructed marine Tl mass balance yields a residence time of ~18.5
852 ka, which is within error of previous estimates of ~21 ka (Flegal and Patterson, 1985;
853 Rehkämper and Nielsen, 2004).

854 The isotope composition of the low-T alteration output is equally difficult to determine.
855 Nielsen et al. (2006c) observed that, in general, the upper oceanic crust is significantly enriched
856 in isotopically light Tl with the shallowest samples displaying the lightest isotope compositions
857 (Fig. 7b). This isotopic signature was interpreted to reflect closed system isotope fractionation
858 during uptake of Tl from seawater, which gradually becomes more depleted in Tl as it penetrated
859 deeper into the oceanic crust. As shown by a Rayleigh fractionation model in which an isotope
860 fractionation factor of $\alpha = 0.9985$ was applied (Nielsen et al., 2006c), the isotope composition of
861 the total Tl deposited during low-T alteration depends critically on the fraction of Tl that is
862 extracted from the seawater before it is re-injected into the oceans as a low-T hydrothermal fluid.
863 Stripping the fluid of all Tl originally present would imply an isotope composition for the low-T
864 alteration flux that is identical to seawater ($\varepsilon^{205}Tl = -6$), whilst lower degrees of depletion result
865 in lighter isotope compositions.

Based on the isotope fractionation observed for rocks from ODP Hole 504B, it was estimated that extraction of ~50% of the original seawater Tl by ocean crust alteration would yield an average isotope composition of $\varepsilon^{205}Tl \sim -18$ for the Tl deposited during low-T alteration. The application of this approach to obtain a global estimate for the average Tl isotope composition of the low-T alteration flux is fraught with many uncertainties, however, as the database is currently limited to rocks from just three sections of altered ocean crust (504B, 801C, U1301B) and Tl concentration measurements for 3 low-T fluids from the Juan de Fuca ridge (Nielsen et al., 2006c). In principle, average altered upper ocean crust can be characterized by an $\varepsilon^{205}Tl$ value of between about -18 to -6. Hence it may again be more appropriate to apply an isotope mass balance approach to obtain a more accurate result. With an isotope composition of $\varepsilon^{205}Tl \approx -1.8$ for the combined marine Tl input fluxes and an authigenic output flux of $\varepsilon^{205}Tl \approx +10$, mass balance dictates that the altered basalt flux is characterized by $\varepsilon^{205}Tl \approx -7.2$ (Table 4). This result is certainly within the range of reasonable values but based on Rayleigh fractionation modeling it requires that more than 95% of seawater Tl is removed by alteration processes, which is not fully supported by the data obtained for ODP Hole 504B (Nielsen et al., 2006c) and IODP Hole U1301B (Coggon et al., 2014). It is unlikely, however, that the results obtained for these two relatively young (<5Ma) sections of oceanic crust are representative for global average ocean crust alteration processes. On the other hand, the Jurassic oceanic crust at ODP Hole 801C was found to have only limited Tl enrichment. This may reflect the low Tl concentration of ambient seawater at the time, as a consequence of enhanced incorporation of Tl into the abundant euxinic sediments of the Jurassic and Cretaceous, during which most of the alteration at ODP 801C took place (Prytulak et al., 2013).

7. CAUSES OF THALLIUM ISOTOPE FRACTIONATION

In general, Tl isotope variations on Earth are fairly limited, with only a few environments displaying significant deviations from the MORB and continental crust value of $\varepsilon^{205}Tl = -2$ (Nielsen et al., 2007; Nielsen et al., 2006b; Nielsen et al., 2005b; Nielsen et al., 2006c). However, the overall magnitude of Tl isotope variations in natural environments on Earth now exceeds 35 ε^{205}Tl-units (Coggon et al., 2014; Nielsen et al., 2006c; Rehkämper et al., 2004; Rehkämper et al., 2002). This variability is substantially larger than what is expected based on classical stable isotope fractionation theory (Bigeleisen and Mayer, 1947; Urey, 1947) and it is therefore important to understand the fundamental processes responsible for the Tl isotope variability.

There are two principle mechanisms by which most stable isotope fractionations are generated – a kinetic route that is associated with unidirectional processes and an equilibrium pathway, which acts during chemical exchange reactions. Both mechanisms should scale with the relative mass difference between the two isotopes of interest. In principle, kinetic isotope fractionation is capable of generating substantial Tl isotope effects (see Section 5.1) and there is evidence that such processes are recorded in volcanic fumaroles and some meteorites (Baker et al., 2009; Baker et al., 2010b; Nielsen et al., 2006a). However, the large Tl isotope fractionations observed between seawater and Fe-Mn oxy-hydroxides are more likely to reflect equilibrium isotope effects (Nielsen et al., 2006c; Rehkämper et al., 2002).

The larger-than-expected Tl isotope effects of equilibrium reactions were shown by Schauble (2007) to be partially caused by the so-called nuclear field shift isotope fractionation mechanism (Bigeleisen, 1996). In short, the fundamental equilibrium isotope exchange equation of Bigeleisen and Mayer (1947) has five components, of which four were deemed negligible.

912 However, based on unusual isotope fractionation effects observed for uranium (Fujii et al.,
913 1989a; Fujii et al., 1989b), it was concluded that the equilibrium term caused by nuclear field
914 shifts may be important in some cases (Bigeleisen, 1996). Thus, nuclear field shift isotope
915 fractionation is also an equilibrium isotope fractionation term, with a magnitude that scales
916 broadly with the mass of the isotopes and hence is largest for heavy elements (Knyazev and
917 Myasoedov, 2001; Schauble, 2007). The calculations that were carried out for Tl isotopes predict
918 that an equilibrium system with aqueous dissolved Tl^{+} and Tl^{3+} will feature both regular mass
919 dependent and nuclear field shift isotope effects, with isotope fractionation factors that act in the
920 same direction (Schauble, 2007). When combined, these two components can reproduce the
921 approximate magnitude of Tl isotope variation observed on Earth (Schauble, 2007). The
922 calculations are particularly relevant for the isotope compositions determined for Fe-Mn crusts
923 and low-T altered basalts as these represent the heaviest and lightest reservoirs, respectively,
924 found to date. The main requirement for substantial equilibrium Tl isotope fractionation to take
925 place, is a chemical exchange reaction that involves two valence states of Tl (Schauble, 2007),
926 and these could be Tl^{0}, Tl^{+} or Tl^{3+}. However, the calculations of Schauble (2007) also imply that
927 the largest isotope effects are expected if Tl^{3+} is present.
928 Based on these theoretical considerations, experimental work was conducted to investigate
929 the mechanism for Tl isotope fractionation during adsorption onto hydrogenetic Fe-Mn crusts
930 (Fig. 8) and other Fe-Mn sediments (Nielsen et al., 2013; Peacock and Moon, 2012). The
931 majority of Tl in these deposits is associated with MnO_2 minerals (Koschinsky and Hein, 2003;
932 Peacock and Moon, 2012) and the isotope fractionation is therefore likely to occur at or in such
933 phases. The EXAFS/XANES spectra for Tl sorbed onto Mn-oxides have shown that the MnO_2
934 phase hexagonal birnessite has the capacity to oxidize Tl^{+} to Tl^{3+}, following Tl sorption as a

935 univalent ion (Bidoglio et al., 1993; Peacock and Moon, 2012). This reaction appears to be
936 associated with isotope fractionation whereas sorption of Tl onto other MnO_2 mineral structures
937 (e.g., todorokite) with less oxidation potential, is not associated with significant isotope effects
938 (Nielsen et al., 2013). Several series of experiments revealed that Tl sorbed to birnessite is
939 systematically enriched in ^{205}Tl (Nielsen et al., 2013), which is in agreement with Tl isotope data
940 for Fe-Mn crusts and seawater (Owens et al., 2016; Rehkämper et al., 2002). However, the
941 experimental isotope fractionation factors measured for aqueous univalent Tl versus Tl sorbed to
942 birnessite were more variable and lower than the constant isotopic fractionation observed
943 between Fe-Mn crusts and seawater (Fig. 8). This discrepancy was interpreted to reflect sorption
944 of Tl to two distinct sorption sites on birnessite: one associated with significant isotope
945 fractionation and one with little or none. If this interpretation is correct, then Tl in natural Fe-Mn
946 crusts either occupies only sorption sites with isotope fractionation or the distribution of Tl
947 between the two types of sites is fairly constant in nature.
948 In summary, observation (Rehkämper et al., 2002), theory (Schauble, 2007) and
949 experiments (Nielsen et al., 2013) provide a relatively consistent picture of the mechanism
950 responsible for Tl isotope fractionation during sorption to Mn oxides. However, it is still
951 unknown what effects, if any, there are on the magnitude of Tl isotope fractionation during
952 sorption to Mn oxides as a function of temperature, pH, ionic strength or other parameters.
953 The isotope fractionation effects found in low-T altered ocean crust are much less well
954 understood. In this environment, Tl is extracted from seawater circulating through the ocean
955 crust with an isotope fractionation factor of about $\alpha = 0.9985$ (Coggon et al., 2014; Nielsen et al.,
956 2006c). It is conceivable that these fractionations reflect kinetic isotope effects, for example as a
957 result of more rapid diffusion of the light isotopes from the hydrothermal fluid to the alteration

958 minerals that concentrate Tl. If an equilibrium reaction is responsible, Tl^{3+} is likely to be
959 involved because large equilibrium isotope effects are not expected for reactions without this
960 species (Schauble, 2007). Simple models of Tl speciation in seawater predict that only Tl^{+} is
961 present (Nielsen et al., 2009a) and this implies that the hydrothermal processes, which deposit Tl
962 in the oceanic crust should produce Tl^{3+}. This inference is in accord with the observation that
963 Tl^{3+} has a much lower aqueous solubility than Tl^{+} (Nriagu, 1998) and this implies that trivalent
964 Tl should be deposited during hydrothermal alteration. However, these conclusions strongly
965 contradict observations, which demonstrate that low-T hydrothermal alteration generally occurs
966 at conditions that are more reducing than those prevalent in the open ocean (Alt et al., 1996). In
967 addition, isotope fractionation calculations indicate that oxidized Tl should be enriched in ^{205}Tl
968 (Schauble, 2007), which is at odds with the light Tl isotope signatures observed in altered
969 basalts.

970 In summary, the large Tl isotope variability observed in the marine environment is most
971 likely produced by a combination of conventional mass dependent and nuclear field shift
972 equilibrium isotope fractionation processes. Contributions from kinetic isotope effects are also
973 possible, but primarily for Tl incorporation during low-T ocean crust alteration. In order to
974 reproduce the magnitude of equilibrium isotope fractionation observed for natural samples,
975 reduction-oxidation processes, in which oxidized Tl^{3+} plays a central role, are predicted to be
976 important.
977

8. APPLICATIONS OF THALLIUM ISOTOPES

8.1. Studies of Tl isotopes in Fe-Mn crusts

Hydrogenetic Fe-Mn crusts grow on hard substrates that experience little or no regular detrital sedimentation, for example on seamounts where ocean currents prevent gravitational settling of particles (Hein et al., 2000). They precipitate directly from the ambient water mass in which they are bathed and feature growth rates of a few mm/Ma (Eisenhauer et al., 1992; Segl et al., 1989; Segl et al., 1984). This implies that samples with a thickness exceeding 10 cm may provide a continuous seawater record for the entire Cenozoic (the last ~65 Ma). Over the last 20 years, extensive investigations of Fe-Mn crusts have been conducted to infer changes in the radiogenic isotope compositions of various elements in deep ocean waters (e.g. Frank, 2002; Lee et al., 1999). Depending on the marine residence time for the element investigated, the isotopic variability has mainly been interpreted as reflecting changes in ocean circulation patterns or the marine source and/or sink fluxes (Burton et al., 1997; van de Flierdt et al., 2004).

The globally uniform Tl isotope compositions observed for the surfaces of Fe-Mn crusts (Fig. 8), imply a constant equilibrium isotope fractionation between seawater and Tl incorporated into the Fe-Mn crusts. Time-dependent variations of Tl isotope compositions in Fe-Mn crusts can be interpreted to reflect either changes in the isotope fractionation factor between seawater and Fe-Mn crusts or the Tl isotope composition of seawater. In principle, both interpretations are feasible, but several lines of reasoning currently favor the latter explanation (Nielsen et al., 2009a; Rehkämper et al., 2004).

Two studies have determined Tl isotope depth profiles for several Fe-Mn crusts, and both identified large systematic changes in Tl isotope compositions (Nielsen et al., 2009a; Rehkämper et al., 2004). The first study produced low-resolution depth profiles for a number of samples. The

1001 largest Tl isotope variations were observed for the early Cenozoic (Rehkämper et al., 2004), but
1002 the low sampling density and uncertainties in the age models of the crusts precluded a precise
1003 determination of the timing and duration of the observed changes. It was furthermore argued that
1004 the Fe-Mn crusts record variations in the Tl isotope composition of seawater that were caused by
1005 changes in the marine input and/or output fluxes of this element (Rehkämper et al., 2004). The
1006 second study generated high resolution Tl isotope time series for two Fe-Mn crusts. Improved
1007 age models were applied, which resolved a single large shift in Tl isotope composition, which
1008 occurred between ~55 and ~45 Ma (Fig. 9; (Nielsen et al., 2009a)). Based on an improved
1009 understanding of the marine input and output fluxes of Tl and their respective isotope
1010 compositions, it was proposed that the large shift in the ε^{205}Tl value of seawater reflects a
1011 decrease in the amount of authigenic Mn oxides that were deposited with pelagic sediments in
1012 the early Eocene (Nielsen et al., 2009a).

1013 It is difficult to assess the underlying mechanism responsible for this global change in Mn
1014 oxide precipitation. The strong co-variation of the Tl isotope curve with the sulfur (S) isotope
1015 composition of seawater (Fig. 9) may imply, however, that the same mechanism is driving the
1016 shift in the isotopic evolution of both stable isotope systems, even though S isotopes are known
1017 to be unaffected (at least directly) by changes in Mn oxide precipitation. Baker et al. (2009)
1018 proposed that the inferred high Mn oxide precipitation rates for the Paleocene (~65-55 Ma) may
1019 be explained by increased deposition of Fe- and Mn-rich volcanic ash particles in the oceans.
1020 Such volcanic activity would also supply isotopically light S and this could explain the relatively
1021 low δ^{34}S value for seawater at this time. The changes in the Tl and S isotope compositions of the
1022 oceans between ~55 and ~45 Ma (Fig. 9) would then be controlled by diminishing volcanic
1023 activity (Wallmann, 2001). An alternative model proposes that Mn oxide precipitation is

1024 controlled by biological utilization and burial of Mn with organic carbon (Nielsen et al., 2009a).
1025 Higher organic carbon burial rates would lead to diminished Mn oxide precipitation rates as less
1026 Mn would be available in the water column. Simultaneously, the increased organic carbon burial
1027 would result in higher rates of sedimentary pyrite burial, which draws isotopically light S out of
1028 seawater (Berner, 1984). In summary, the results of initial paleoceanographic studies indicate
1029 that it may be possible to utilize Tl isotopes as a proxy for changes in marine Mn sources and/or
1030 Mn oxide precipitation rates back in time.
1031

1032 **8.2. Calculation of hydrothermal fluid fluxes using Tl isotopes in the ocean crust**

1033 Hydrothermal fluids are expelled from the seafloor (i) at high temperature on mid ocean
1034 ridge axes, as fueled by the magmatic energy from the crystallization and cooling of newly
1035 produced ocean crust to ~300-400°C and (ii) at lower temperatures on the ridge flanks, as the
1036 ocean crust cools further over millions of years. These hydrothermal fluxes play pivotal roles in
1037 controlling seawater chemistry, but the magnitude of the high temperature water flux at mid-
1038 ocean ridge axes remains widely disputed, whilst the volume of low temperature vent fluids
1039 expelled at ridge flanks is essentially unconstrained.

1040 As discussed in sections 6.1.1 and 6.2.2, Tl displays distinct behavior during high and low
1041 temperature hydrothermal alteration of the ocean crust. High-T fluids effectively leach Tl from
1042 the cooling rocks whereas low-T fluids deposit Tl into the upper part of the oceanic crust.
1043 Following Nielsen et al. (2006c), a mass balance equation can be constructed for the high-T
1044 hydrothermal fluid flux (F_{hT}):

1045 $$F_{hT} \times [Tl]_{hT} = M_{Tl} \quad (3)$$

where $[Tl]_{hT}$ is the average Tl concentration of the vent fluids and, as defined in equation (2), M_{Tl} is the annual flux of Tl expelled into the ocean via high-T hydrothermal fluids. When the Tl flux of 170±60 Mg/a determined from equation (2) is combined with $[Tl]_{hT}$ = 6.7±0.7 ng/g (Nielsen et al., 2006c), we obtain a high temperature hydrothermal water flux of 2.5±0.9 x 10^{13} kg/a. This fluid flux corresponds to 50-80% of the heat available at mid-ocean ridge axes from the crystallization and cooling of the freshly formed ocean crust (Mottl, 2003). The difference between the available heat at mid-ocean ridge axes and that expelled via hydrothermal fluids requires that some energy at mid ocean ridge axes is lost via conduction and/or through the circulation of intermediate temperature hydrothermal fluids that do not alter the chemical budgets of Tl in the ocean crust (Nielsen et al., 2006c).

For the low-T hydrothermal fluid circulation flux (F_{lT}), the following mass balance equation was shown to apply (Nielsen et al., 2006c):

$$F_{vz} \times ([Tl]_{avz} - [Tl]_{pvz}) = F_{lT} \times [Tl]_{sw} \times f_{upt} \quad (4)$$

where F_{vz} is the mass flux of newly produced ocean crust that is affected by low-T alteration, $[Tl]_{avz}$, $[Tl]_{pvz}$, and $[Tl]_{sw}$ are the Tl concentrations of the altered volcanic zone basalts, their pristine equivalents and seawater, respectively. The fraction of Tl that is removed from seawater by basalt weathering is denoted by f_{upt}. As discussed in section 6.2.2, $[Tl]_{avz}$ is extremely difficult to assess because the oceanic crust at ODP Holes 504B, 896A and U1301B is younger than 5Ma, which means that hydrothermal alteration is still ongoing at these locations. Analyses of Jurassic oceanic crust at ODP Hole 801C revealed little to no Tl enrichment (Fig. 7), possibly due to much lower Tl concentrations in seawater at the time (Prytulak et al., 2013). A meaningful assessment of Tl accumulation in oceanic crust that experienced complete hydrothermal alteration is hence currently not possible. The Tl enrichment factors observed for rocks from drill

holes in young oceanic crust (Fig. 7) are, therefore, likely minimum estimates. The remaining parameters are more easily determined, but the large uncertainty on $[Tl]_{avz}$ generates estimates for the low-T hydrothermal fluid fluxes at ridge flanks that are also highly uncertain at 0.2-5.4 x 10^{17} kg/a (Nielsen et al., 2006c). Using the ridge flank power output of 7.1 TW (Mottl, 2003), it was calculated that such fluids have an average temperature anomaly of only about 0.1 to 3.6°C relative to ambient seawater, which is lower than most flank fluids sampled to date. It is therefore unclear how representative low-T fluids sampled to date are of average low-T ocean crust alteration processes.

In order to improve the utility of Tl mass balance calculations to constrain hydrothermal fluid fluxes it will be essential to obtain more data on altered ocean crust from a number of locations and particularly for older sections of altered oceanic crust. However, Jurassic ocean crust appears to not follow the general pattern of strong Tl enrichment during low-T alteration and this may reflect the particular marine conditions of this era (Prytulak et al., 2013). Analyses of intermediate-age altered oceanic crust (20-100Ma) will provide improved constraints on the behavior of Tl during hydrothermal processes and may thus ultimately yield more reliable Tl-based estimates of global hydrothermal water fluxes.

8.3 High temperature terrestrial applications

8.3.1 Mineral Deposits

The accumulation of Tl via hydrothermal activity and the association of Tl and S, suggests obvious potential applications for Tl elemental systematics and isotope signatures in mineral deposit exploration. The significantly elevated concentrations of Tl in many mineral deposits furthermore allows analyses of mineral separates, which are often at the limits of analytical

1092 capabilities in barren igneous systems. Such investigations provide useful information on the
1093 magnitude and direction of natural mineral fractionation factors. For example, it is of interest to
1094 determine if Tl-enriched minerals have a distinctive Tl isotope 'fingerprint' that could dominate
1095 bulk rock assays and thus aid exploration activities.

1096 The first economically focused study of thallium and thallium isotopes was undertaken by
1097 Baker et al. (2010a), who investigated a porphyry copper deposit hosted in the Collahuasi
1098 Formation of northern Chile. These authors examined whole rock andesite, dacite, rhyolite and
1099 Cu-porphyry samples. The concentration of thallium was found to vary over an order of
1100 magnitude from 0.1 to 3.2 μg/g, correlating with K and Rb, and not Cu, thus indicting that Tl
1101 displays lithophile rather than chalcophile behavior in this system (Baker et al., 2010a). The
1102 isotope compositions ranged from $\varepsilon^{205}Tl$ = -5.1 to +0.1, which is not unusual in terms of the
1103 range of $\varepsilon^{205}Tl$ seen in barren terrestrial igneous rocks (Fig. 1). The five examined porphyry
1104 samples had very restricted $\varepsilon^{205}Tl$ values of -1.9±0.1, identical to $\varepsilon^{205}Tl_{MORB}$. Thus there appears
1105 little potential for fingerprinting Cu porphyry rocks with Tl isotopes. Furthermore, there were no
1106 clear, systematic relationships between $\varepsilon^{205}Tl$ and major and trace element data or alteration
1107 minerals, which also limits the diagnostic potential for Tl isotopes in Cu porphyry systems.

1108 Hettmann et al. (2014) addressed the magnitude of Tl isotope fractionation between different
1109 sulfide melts by examining the Pb-As-Tl-Zn deposit at the Lengenbach quarry in Switzerland.
1110 The Lengenbach deposit is notable for its abundance of rare Tl-bearing minerals, including
1111 hatchite ($AgTlPbAs_2S_5$) with an extreme thallium concentration of up to 24.8 wt%. The high
1112 concentrations of Tl in the ore minerals allowed isotopic analysis of individual mineral phases
1113 and thus an evaluation of potential isotope fractionation induced by sulfide melt/mineral
1114 partitioning. The overall range of $\varepsilon^{205}Tl$ measured in sulfides, sulfosalts and micas spans $\varepsilon^{205}Tl$ =

-4.1 to +1.9. As for the Collahuasi deposit, the substantial range in Tl isotope compositions over a geographically restricted area was not accompanied by a clear co-variation with other chemical characteristics or mineralogy. Complicated processes including both hydrothermal and sulfide melt inputs and subsequent formation and dissolution of secondary phases are likely responsible for the general lack of coherent behavior. Certainly, the Tl concentrations documented are amongst the highest measured in natural materials, yet the isotopic variability, whilst large, is again within the range of barren igneous rocks.

Given the significant and resolvable variability in ε^{205}Tl for both examined deposits, there is clearly much to be explored in terms of individual mineral controls on isotope signatures and the potential effects of fluid mineral partitioning at different pH, fO_2 and T. The utility of Tl isotopes to fingerprint economically viable deposits, however, remains to be convincingly demonstrated.

8.3.2 The Tl isotope composition of arc lavas

Subduction related magmas are classically considered to be derived from a depleted mantle wedge, chemically flavored by percent-level addition of sediments and/or fluids released from the subducting slab. Due to the large diversity of Tl concentrations and isotope compositions among these three reservoirs (Fig. 1), Tl isotopes appear to be uniquely suited to disentangle these sources and investigate the petrogenesis of subduction-related lavas. Although back arc spreading may cause the mantle wedge to be more depleted than the source of mid-ocean ridge basalts, to a first order, the depleted upper mantle is a reasonable estimate for the Tl content and isotope composition of the mantle wedge. The Tl concentration of the depleted mantle is orders of magnitude lower than possible inputs to the system in the form of sediments and fluids from the altered oceanic crust (Fig. 1). In addition to the large concentration contrast between

1138 'background' mantle and possible inputs, the two most commonly invoked inputs have opposite
1139 vectors of isotope fractionation. As discussed in sections 6.2.1 and 6.2.2, pelagic sediments rich
1140 in Mn oxides are characterized by positive ε^{205}Tl whilst altered oceanic crust and, by inference,
1141 slab fluids derived thereof are expected to yield negative ε^{205}Tl signatures. Thus, even minor
1142 addition of Mn oxide rich sediments or low-T altered basalts to a mantle wedge can result not
1143 only in analytically resolvable Tl isotope signatures, but also identify the type of input a specific
1144 lava has experienced. Finally, Tl isotope measurements may be able to contribute to the debate
1145 over the petrogenesis of so-called 'adakite' lavas (Kay, 1978), whereby one long-standing
1146 hypothesis proposes that they are produced by direct melting of the (altered) basaltic portion of
1147 the subducting slab.

1148 The prediction is straightforward: lavas with trace element chemistry indicative of fluid
1149 contributions are expected to have light Tl isotope signatures, whilst sediment-influenced lavas
1150 are expected to be isotopically heavy. However, Tl isotope measurements of lavas from the
1151 Mariana subduction zone display very little isotopic variation, with ε^{205}Tl values from -1.8 to -
1152 0.4. One lava falls outside this range, with a heavy ε^{205}Tl of +1.2, which was suggested to be
1153 due to volcanic degassing (Prytulak et al., 2013). Hence, even though volcanic degassing broadly
1154 speaking has little impact on the Tl isotope composition of lavas and the continental crust (see
1155 section 5.1), individual samples may be affected by this process and must be assessed in studies
1156 of subaerial volcanism. The remaining data from the Mariana arc are reasonable, in that the
1157 measured inputs to the system, including sediments and altered ocean crust from ODP Hole
1158 801C, did not show the same variability of Tl isotope compositions that was documented in
1159 similar lithologies elsewhere. In addition, a subsequent study of Mariana forearc serpentinites
1160 revealed that Tl sourced from pelagic sediments was released with fluids from the subducting

1161 sediments that caused serpentinization of the forearc peridotites (Nielsen et al., 2015). This result
1162 suggests that the Tl isotope signature of subducting sediments may be altered in the forearc
1163 before they enter the subarc mantle. This process could be an important mechanism of
1164 subduction zone cycling for Tl and other trace metals that concentrate in Mn oxides. In
1165 summary, the Tl isotope data for Mariana arc lavas demonstrates a situation where isotopically
1166 invariant inputs produce similarly invariant outputs. This is a key finding, as it provides
1167 evidence that the subduction process itself does not fractionate Tl isotopes (Prytulak et al., 2013).
1168 The only other subduction zone that has been investigated for Tl isotopes is the Aleutian arc
1169 (Nielsen et al., 2016). The Aleutians are notable for along strike variation in subduction
1170 parameters, such as slab dip, slab velocity, and variable sediment lithologies dominated by
1171 volcaniclastic in the East to pelagic clay in the West. In addition, the Aleutians contain the type
1172 locality for so-called adakite lavas, from Adak Island, Alaska. Nielsen et al. (2016) analyzed
1173 both lavas and sedimentary lithologies outboard of the arc and demonstrated that the ε^{205}Tl
1174 values of the lavas closely follow the sediment values, whereby the latter change systematically
1175 along the arc, with the Central Aleutian sediments and lavas showing enrichments in ^{205}Tl
1176 relative to the Eastern Aleutians. This finding further strengthens the conclusion that subduction
1177 processes do not fractionate Tl isotopes and which are thus useful for tracing inputs that are
1178 isotopically distinct from the background mantle. Nielsen et al. (2016) also determined the Tl
1179 isotopic composition of the lava originally used to define adakites (Defant and Drummond, 1990;
1180 Kay, 1978). As expected, the sample has a light ε^{205}Tl of -3.3, in general agreement with the
1181 hypothesis that adakites incorporate melts from the altered basaltic ocean crust (Nielsen et al.,
1182 2016).
1183

8.3.3 The Tl isotope composition of ocean island basalts (OIB)

The recycling of sediments and oceanic crust is a central tenant of mantle geochemistry and has been the subject of intense research over the past 35 years (e.g. Hofmann, 2014). Many investigations focus on ocean island basalts, which are argued to be generated at pressures >2.5GPa in the mantle, and thus significantly deeper than mid-ocean ridge basalts. Though still debated, there is some consensus that many ocean island basalts are produced by anomalously hot mantle plumes, thus offering a reasonable explanation why their locations are independent of tectonic plate boundaries (Hofmann, 2014; Hofmann and White, 1982). Traditional approaches to deduce the nature of OIB mantle sources employ a combination of trace element and radiogenic isotope data to distinguish sediment and/or crustal additions. As radiogenic isotopes reflect the time-integrated parent–daughter trace element ratio, there is inescapable ambiguity associated with their employment, with the same isotope signature permissibly generated by markedly different evolution paths.

Stable isotope analyses offer important complementary constraints to measurements that apply radiogenic isotope systems. Some of the earliest applications of stable isotopes to high temperature geochemistry encompass studies of O and Li to trace processes such as ocean crust alteration (Alt et al., 1986; Chan et al., 2002). However, light elements like O and Li are known to record isotope fractionation even during processes that occur at elevated mantle temperatures (Jeffcoate et al., 2007; Marschall et al., 2007; Williams et al., 2009) and their mantle concentrations are relatively high, such that the isotope composition of a mantle source is not readily affected by admixing of sediment and/or ocean crust (Elliott et al., 2004; Thirlwall et al., 2004). However, the concentration contrast and magnitude of isotope fractionation offered by the Tl isotope system is favorable for overcoming these obstacles.

To date, OIB samples from the Azores, Iceland and Hawaii have been investigated (Nielsen et al., 2007; Nielsen et al., 2006b). As it is unclear whether the Azores basalts were affected by post-eruptional alteration (Nielsen et al., 2007), these data will not be discussed in the following. Samples from Hawaii exhibit the most convincing Tl isotope evidence for the presence of sediments in the mantle source (Fig. 10). In detail, about 8 ppm of pure Fe-Mn sediment is sufficient to explain the positive ε^{205}Tl values of up to +4 recorded in these lavas. Whilst it is unlikely that the Tl isotope variation originates from anything else than Fe-Mn sediment, it is uncertain if this component was acquired by the melts during magma ascent via assimilation of modern marine deposits or if it is a feature of the mantle source. The samples with the heaviest Tl isotope compositions are, however, also characterized by the least radiogenic Pb isotope compositions (Nielsen et al., 2006b) which would argue for an old age of the sedimentary component.

The relatively straightforward interpretation of the Tl isotope data for Hawaii could be considered a "smoking gun" for the presence of recycled sediments in the Hawaiian mantle plume and, indeed, agrees with independent constraints from Hf isotopes (Blichert-Toft et al., 1999). However, results obtained for of a suite of lavas from Iceland strongly indicate that there is some way to go before Tl isotopes can be confidently applied as a unique tracer of crustal recycling within the mantle. Seventeen Icelandic samples, including picrites that span all major eruption centers of the island, exhibit an average $\varepsilon^{205}\text{Tl} = -1.6 \pm 1.1$, completely overlapping with $\varepsilon^{205}\text{Tl}_{\text{MORB}}$. In contrast to the isotopic homogeneity, Cs/Tl ratios vary from 0.3 to 11. The isotopic invariance is perhaps unsurprising given that the thickness of subducted oceanic lithosphere exceeds 30km. Thallium isotope anomalies will be situated in only the uppermost ~500 to 1000m, whilst the remainder of the oceanic crust is expected to be isotopically identical

to the ambient mantle. The mantle-like Tl isotope signatures of the Iceland basalts hence do not argue against the presence of recycled ocean crust in the plume source. Of more concern is that the samples display variable Cs/Tl ratios. The large observed Cs/Tl range demonstrates that processes other than the addition of Fe-Mn sediments and low-T altered basalts may alter this ratio. It is conceivable that this includes igneous processes, such as partitioning of Tl into sulfides and/or phyllosilicates, Tl mobilization by magmatic fluids (Nielsen et al., 2007) and/or fractionation by accessory phases in the subducted material (e.g., phengite; (Prytulak et al., 2013)).

Finally, it is prudent to consider three key caveats for the application of Tl isotopes in mantle geochemistry. First, it is likely that the Tl isotope composition of seawater has not remained constant over time (Fig. 9) and the isotope signatures of altered basalts and Fe-Mn sediments are therefore also expected to exhibit temporal variability. Any such variability will obscure the mixing trends that are produced by contamination of the ambient mantle with recycled material. Second, whilst it is unclear when the oceans became sufficiently oxic to support the precipitation of Mn oxides, this probably occurred after ~2.4 Ga (Canfield, 1998). Sediments that were recycled more than 2.4 billion years ago are therefore unlikely to be enriched in Tl associated with Mn oxides and are hence probably characterized by $\varepsilon^{205}Tl \approx -2$. The isotope fractionation mechanism responsible for the highly negative $\varepsilon^{205}Tl$ values of modern altered ocean crusts is yet to be determined. Hence, it is unclear whether such basalts are also isotopically fractionated in ancient environments and if past oceanic crust recycling was able to alter the Tl isotope composition of the mantle. Third, it needs to be acknowledged that Tl can also be *too* sensitive as a tracer. Even much less than 1% of subaerial or submarine contamination by secondary clays or precipitation of Mn oxides can have a drastic impact on the

1253 Tl concentration and isotope signature of a basalt. Great attention must therefore be paid to
1254 sample preparation and selection. For example, the careful leaching experiments for submarine
1255 samples conducted by Nielsen et al. (2016) should be considered a minimum requirement to
1256 establish confidence in the determined ε^{205}Tl isotope signatures of submarine lavas with low Tl
1257 concentrations.
1258
1259 **9. FUTURE DIRECTIONS AND OUTLOOK**
1260 High precision measurements of Tl isotope compositions have only been possible for little
1261 more than a decade but despite of this, we have already acquired a surprisingly detailed
1262 understanding of the diverse isotopic behavior of this element. Significant gaps in knowledge
1263 remain, however.
1264 Most meteorite samples display resolvable variations in Tl isotope compositions with an
1265 overall isotopic variability of about 50 ε^{205}Tl. In many samples, the isotopic variation appears to
1266 be caused by both radiogenic decay of extinct ^{205}Pb and stable isotope fractionations, which
1267 reflect the highly volatile and labile nature of Tl. The difficulty of deconvolving these two
1268 sources of isotopic variability restricts the utility of both the ^{205}Pb-^{205}Tl chronometer and the Tl
1269 stable isotope system to inform on early solar system processes. Nonetheless, further studies of
1270 suitable meteorites (including carbonaceous chondrites) are desirable to better constrain the
1271 initial solar system abundance of ^{205}Pb, as this is a unique tracer of freshly synthesized s-process
1272 material that was delivered to the nascent solar system.
1273 For the Earth, it is desirable to further expand the Tl isotope and concentration database for
1274 various environments, in order to gain a better understanding of the geochemical distribution and

cycling of this element. In addition, there are a few crucial investigations that are needed to advance the utility of Tl isotopes as quantitative tracers of past and present geological processes.

First of all, we must fully understand the mechanisms that govern the two major Tl isotope effects observed on Earth, which produce highly fractionated Tl isotope signatures in marine Mn oxides and low-T altered basalts. Experimental studies have shown that Tl oxidation and adsorption to the Mn oxide birnessite is clearly the central processes responsible for the heavy isotope ratios recorded in Mn oxide rich marine sediments (Nielsen et al., 2013; Peacock and Moon, 2012). However, the magnitude of isotope fractionation and the effect of changes in intensive parameters like T, redox potential and ionic strength are presently unknown. Further studies of both natural and synthetic systems that mimic the conditions of Mn oxide precipitation and low-T ocean crust alteration are required to establish the mechanisms controlling Tl isotope fractionation in these two critical reservoirs. This knowledge will not only help expand our appreciation of the physico-chemical processes that cause isotope fractionation in heavy elements, but also enable us to better utilize the Tl isotope system to quantify low-T hydrothermal fluid flow (Nielsen et al., 2006c) and help to unravel the causes of the Tl isotope variations observed in the marine environment over time (Baker et al., 2009; Nielsen et al., 2009a).

Furthermore, it will be important to refine the three applications outlined in section 8. For the paleoceanographic studies, this will include a detailed determination of the magnitude and isotope compositions of the most uncertain marine Tl fluxes. These are the fluxes associated with benthic pore waters, adsorption processes on pelagic clays and low-T hydrothermal alteration. A complete understanding of the modern marine Tl cycle is a prerequisite for good models of past Tl isotope variations. Another aspect of the oceanic Tl isotope evolution that has yet to be

investigated are short-term fluctuations, for example on glacial-interglacial time-scales or ocean anoxic events. Since the marine residence time of Tl is about 18.5 ka (Table 4), it should be feasible to observe perturbations of the Tl cycle that occur on geologically rapid time-scales. To this end, a recent study of Tl isotopes in euxinic sediments has revealed no detectable isotope fractionation between seawater and sediment (Owens et al., 2016). This is an important result because such sediments may now enable reconstruction of marine Tl isotope signatures in deep time.

The use of Tl isotopes as a tool in mantle geochemistry is currently limited by scant data. Thallium isotope and concentration data are presently available only for a few OIB and there is a lack of understanding concerning how Tl is cycled through subduction zones. Recent studies that attempted to address such questions through Tl isotope analyses of cratonic eclogites (Nielsen et al., 2009b) and island arc lavas (Nielsen et al., 2016; Prytulak et al., 2013) were unable to conclusively constrain the behavior of Tl and further investigations of rocks from subduction related environments are thus necessary.

The application of Tl isotopes as a tracer of anthropogenic Tl emissions to the environment has been shown to be viable in an initial study (Kersten et al., 2014) and hence shows promise for future investigations. However, whilst Tl is a highly toxic element, it shows low concentrations in most natural materials and is used to only a limited extent in industrial products and processes. Hence, Tl isotopes are unlikely to develop into a widely used tracer of anthropogenic emission, similar to radiogenic Pb isotope compositions, but will be of utility to trace Tl origin and mobility in particular, localized pollution scenarios.

10. REFERENCES

Alleman, L.Y., Veron, A.J., Church, T.M., Flegal, A.R., Hamelin, B., 1999. Invasion of the abyssal North Atlantic by modern anthropogenic lead. Geophys. Res. Lett. 26, 1477-1480.

Alt, J.C., 1995. Subseafloor processes in mid-ocean ridge hydrothermal systems, in: Humphris, S.E., Lupton, J.E., Mullineaux, L.S., Zierenberg, R.A. (Eds.), Seafloor Hydrothermal Systems, Physical, Chemical, and Biological Interactions. AGU, Washington DC, pp. 85-114.

Alt, J.C., Muehlenbachs, K., Honnorez, J., 1986. An oxygen isotopic profile through the upper kilometer of the oceanic crust, DSDP Hole 504B. Earth Planet. Sci. Lett. 80, 217-229.

Alt, J.C., Teagle, D.A.H., Bach, W., Halliday, A.N., Erzinger, J., 1996. Stable and strontium isotopic profiles through hydrothermally altered upper oceanic crust, hole 504B. Proc. ODP Sci. Results 148, 57-69.

Anders, E., Stevens, C.M., 1960. Search for extinct lead 205 in meteorites. J. Geophys. Res. 65, 3043-3047.

Andreasen, R., Rehkämper, M., Benedix, G.K., Theis, K.J., Schönbächler, M., Smith, C.L., 2012. Lead-thallium chronology of IIAB and IIIAB iron meteorites and the solar system initial abundance of lead-205, Lunar and Planetary Science Conference. Lunar and Planetary Institute, Woodlands, TX, p. Abstract #2902.

Andreasen, R., Schönbächler, M., Rehkämper, M., 2009. The Pb-205-(TI)-T-205 and Cd isotope systematics of ordinary chondrites. Geochim. Cosmochim. Acta. 73, A43-A43.

Archer, C., Vance, D., 2008. The isotopic signature of the global riverine molybdenum flux and anoxia in the ancient oceans. Nature Geoscience 1, 597-600.

Arden, J.W., Cressey, G., 1984. Thallium and Lead in the Allende C3v Carbonaceous Chondrite - a Study of the Matrix Phase. Geochim. Cosmochim. Acta. 48, 1899-1912.

Baker, R.G.A., Rehkämper, M., Hinkley, T.K., Nielsen, S.G., Toutain, J.P., 2009. Investigation of thallium fluxes from subaerial volcanism-Implications for the present and past mass balance of thallium in the oceans. Geochim. Cosmochim. Acta. 73, 6340-6359.

Baker, R.G.A., Rehkämper, M., Ihlenfeld, C., Oates, C.J., Coggon, R.M., 2010a. Thallium isotope variations in an ore-bearing continental igneous setting: Collahuasi Formation, Northern Chile. Geochim. Cosmochim. Acta. 74, 4405-4416.

Baker, R.G.A., Schönbächler, M., Rehkämper, M., Williams, H.M., Halliday, A.N., 2010b. The thallium isotope composition of carbonaceous chondrites - New evidence for live Pb-205 in the early solar system. Earth Planet. Sci. Lett. 291, 39-47.

Ballhaus, C., Laurenz, V., Münker, C., Fonseca, R.O.C., Albarede, F., Rohrbach, A., Lagos, M., Schmidt, M.W., Jochum, K.P., Stoll, B., Weis, U., Helmy, H.M., 2013. The U/Pb ratio of the Earth's mantle-A signature of late volatile addition. Earth Planet. Sci. Lett. 362, 237-245.

Ben Othmann, D., White, W.M., Patchett, J., 1989. The geochemistry of marine sediments, island arc magma genesis, and crust-mantle recycling. Earth Planet. Sci. Lett. 94, 1-21.

Berner, R.A., 1984. Sedimentary Pyrite Formation - an Update. Geochim. Cosmochim. Acta. 48, 605-615.

Bidoglio, G., Gibson, P.N., Ogorman, M., Roberts, K.J., 1993. X-Ray-Absorption Spectroscopy Investigation of Surface Redox Transformations of Thallium and Chromium on Colloidal Mineral Oxides. Geochim. Cosmochim. Acta. 57, 2389-2394.

Bigeleisen, J., 1996. Nuclear size and shape effects in chemical reactions. Isotope chemistry of the heavy elements. Journal of the American Chemical Society 118, 3676-3680.

Bigeleisen, J., Mayer, M.G., 1947. Calculation of Equilibrium Constants for Isotopic Exchange Reactions. Journal of Chemical Physics 15, 261-267.

Blake, J.B., Lee, T., Schramm, D.N., 1973. CHRONOMETER FOR S-PROCESS NUCLEOSYNTHESIS. Nature-Physical Science 242, 98-100.

Blichert-Toft, I., Frey, F.A., Albarede, F., 1999. Hf isotope evidence for pelagic sediments in the source of Hawaiian basalts. Science 285, 879-882.

Bruland, K.W., 1983. Trace elements in seawater, in: Riley, J.P., Chester, R. (Eds.), Chemical Oceanography. Acad. Press, London, pp. 157-221.
Burton, K.W., 2006. Global weathering variations inferred from marine radiogenic isotope records. Journal of Geochemical Exploration 88, 262-265.
Burton, K.W., Ling, H.F., Onions, R.K., 1997. Closure of the Central American Isthmus and its effect on deep-water formation in the North Atlantic. Nature 386, 382-385.
Canfield, D.E., 1998. A new model for Proterozoic ocean chemistry. Nature 396, 450-453.
Carlson, R.W., Hauri, E.H., 2001. Extending the Pd-107-Ag-107 chronometer to low Pd/Ag meteorites with multicollector plasma-ionization mass spectrometry. Geochim. Cosmochim. Acta. 65, 1839-1848.
Chan, L.H., Alt, J.C., Teagle, D.A.H., 2002. Lithium and lithium isotope profiles through the upper oceanic crust: a study of seawater-basalt exchange at ODP Sites 504B and 896A. Earth Planet. Sci. Lett. 201, 187-201.
Cheam, V., 2001. Thallium contamination of water in Canada. Water Qual. Res. J. Canada 36, 851-877.
Chen, J.H., Wasserburg, G.J., 1987. A search for evidence of extinct lead 205 in iron meteorites. LPSC XVIII, 165-166.
Chen, J.H., Wasserburg, G.J., 1994. The abundance of thallium and premordial lead in selected meteorites - the search for ^{205}Pb. LPSC XXV, 245.
Coggon, R.M., Rehkämper, M., Atteck, C., Teagle, D.A.H., Alt, J.C., Cooper, M.J., 2014. Mineralogical and Microbial Controls on Thallium Uptake During Hydrothermal Alteration of the Upper Ocean Crust. Geochim. Cosmochim. Acta. 144, 25-42.
Craddock, P.R., Warren, J.M., Dauphas, N., 2013. Abyssal peridotites reveal the near-chondritic Fe isotopic composition of the Earth. Earth Planet. Sci. Lett. 365, 63-76.
Defant, M.J., Drummond, M.S., 1990. Derivation of Some Modern Arc Magmas by Melting of Young Subducted Lithosphere. Nature 347, 662-665.
Eisenhauer, A., Gogen, K., Pernicka, E., Mangini, A., 1992. Climatic Influences on the Growth-Rates of Mn Crusts During the Late Quaternary. Earth Planet. Sci. Lett. 109, 25-36.
Elderfield, H., 1976. Manganese fluxes to the oceans. Mar. Chem. 4, 103-132.
Elliott, T., Jeffcoate, A., Bouman, C., 2004. The terrestrial Li isotope cycle: light-weight constraints on mantle convection. Earth Planet. Sci. Lett. 220, 231-245.
Flegal, A.R., Patterson, C.C., 1985. Thallium concentrations in seawater. Mar. Chem. 15, 327-331.
Flegal, A.R., Sanudo-Wilhelmy, S., Fitzwater, S.E., 1989. Particulate thallium fluxes in the northeast Pacific. Mar. Chem. 28, 61-75.
Frank, M., 2002. Radiogenic isotopes: Tracers of past ocean circulation and erosional input. Rev. Geophys. 40, art. no.-1001.
Fujii, Y., Nomura, M., Okamoto, M., Onitsuka, H., Kawakami, F., Takeda, K., 1989a. An Anomalous Isotope Effect of U-235 in U(IV)-U(VI) Chemical Exchange. Zeitschrift Fur Naturforschung Section a-a Journal of Physical Sciences 44, 395-398.
Fujii, Y., Nomura, M., Onitsuka, H., Takeda, K., 1989b. Anomalous Isotope Fractionation in Uranium Enrichment Process. Journal of Nuclear Science and Technology 26, 1061-1064.
Gale, A., Dalton, C.A., Langmuir, C.H., Su, Y.J., Schilling, J.G., 2013. The mean composition of ocean ridge basalts. Geochem. Geophys. Geosyst. 14, 489-518.
Gauthier, P.J., Le Cloarec, M.F., 1998. Variability of alkali and heavy metal fluxes released by Mt. Etna volcano, Sicily, between 1991 and 1995. J. Volcanol. Geotherm. Res. 81, 311-326.
Genna, D., Gaboury, D., 2015. Deciphering the Hydrothermal Evolution of a VMS System by LA-ICP-MS Using Trace Elements in Pyrite: An Example from the Bracemac-McLeod Deposits, Abitibi, Canada, and Implications for Exploration. Econ Geol 110, 2087-2108.
Heggie, D., Klinkhammer, G., Cullen, D., 1987. Manganese and Copper Fluxes from Continental Margin Sediments. Geochim. Cosmochim. Acta. 51, 1059-1070.

Hein, J.R., Koschinsky, A., Bau, M., Manheim, F.T., Kang, J.-K., Roberts, L., 2000. Cobalt-rich ferromanganese crusts in the Pacific, in: Cronan, D.S. (Ed.), Handbook of Marine Mineral Deposits. CRC Press, Boca Raton, pp. 239-280.
Heinrichs, H., Schulz-Dobrick, B., Wedepohl, K.H., 1980. Terrestrial Geochemistry of Cd, Bi, Tl, Pb, Zn and Rb. Geochim. Cosmochim. Acta. 44, 1519-1533.
Hettmann, K., Kreissig, K., Rehkämper, M., Wenzel, T., Mertz-Kraus, R., Markl, G., 2014. Thallium geochemistry in the metamorphic Lengenbach sulfide deposit, Switzerland: Thallium-isotope fractionation in a sulfide melt. American Mineralogist 99, 793-803.
Hinkley, T.K., Lecloarec, M.F., Lambert, G., 1994. Fractionation of Families of Major, Minor and Trace-Metals Across the Melt Vapor Interface in Volcanic Exhalations. Geochim. Cosmochim. Acta. 58, 3255-3263.
Hofmann, A.W., 2014. Sampling Mantle Heterogeneity through Oceanic Basalts: Isotopes and Trace Elements, in: Heinrich, D.H.a.K.K.T. (Ed.), Treatise on Geochemistry (Second Edition). Elsevier, Oxford, pp. 67-101.
Hofmann, A.W., White, W.M., 1982. Mantle plumes from ancient oceanic crust. Earth Planet. Sci. Lett. 57, 421-436.
Huey, J.M., Kohman, T.P., 1972. Search for extinct natural radioactivity of Pb-205 via thallium-isotope anomalies in chondrites and lunar soil. Earth Planet. Sci. Lett. 16, 401-412.
Huh, Y., Chan, L.H., Zhang, L., Edmond, J.M., 1998. Lithium and its isotopes in major world rivers: Implications for weathering and the oceanic budget. Geochim. Cosmochim. Acta. 62, 2039-2051.
Jeffcoate, A.B., Elliott, T., Kasemann, S.A., Ionov, D., Cooper, K., Brooker, R., 2007. Li isotope fractionation in peridotites and mafic melts. Geochim. Cosmochim. Acta. 71, 202-218.
Jenner, F.E., O'Neill, H.S.C., 2012. Analysis of 60 elements in 616 ocean floor basaltic glasses. Geochem. Geophys. Geosyst. 13.
Jochum, K.P., Verma, S.P., 1996. Extreme enrichment of Sb, Tl and other trace elements in altered MORB. Chem. Geol. 130, 289-299.
Johnson, K.S., Berelson, W.M., Coale, K.H., Coley, T.L., Elrod, V.A., Fairey, W.R., Iams, H.D., Kilgore, T.E., Nowicki, J.L., 1992. Manganese Flux from Continental-margin Sediments in a Transect Through the Oxygen Minimum. Science 257, 1242-1245.
Jones, J.H., Hart, S.R., Benjamin, T.M., 1993. Experimental partitioning studies near the Fe-FeS eutectic, with an emphasis on elements important to iron meteorite chronologies (Pb, Ag, Pd, and Tl). Geochim. Cosmochim. Acta. 57, 453-460.
Kay, R.W., 1978. Aleutian magnesian andesites - melts from subducted Pacific ocean crust. J. Volcanol. Geotherm. Res. 4, 117-132.
Kelley, K.A., Plank, T., Ludden, J., Staudigel, H., 2003. Composition of altered oceanic crust at ODP Sites 801 and 1149. Geochem. Geophys. Geosyst. 4.
Kersten, M., Xiao, T.F., Kreissig, K., Brett, A., Coles, B.J., Rehkämper, M., 2014. Tracing Anthropogenic Thallium in Soil Using Stable Isotope Compositions. Environ. Sci. Technol. 48, 9030-9036.
Kiseeva, E.S., Wood, B.J., 2013. A simple model for chalcophile element partitioning between sulphide and silicate liquids with geochemical applications. Earth Planet. Sci. Lett. 383, 68-81.
Knyazev, D.A., Myasoedov, N.F., 2001. Specific effects of heavy nuclei in chemical equilibrium. Separ Sci Technol 36, 1677-1696.
Koschinsky, A., Hein, J.R., 2003. Acquisition of elements from seawater by ferromanganese crusts: Solid phase association and seawater speciation. Mar. Geol. 198, 331-351.
Kruijer, T.S., Fischer-Gödde, M., Kleine, T., Sprung, P., Leya, I., Wieler, R., 2013. Neutron capture on Pt isotopes in iron meteorites and the Hf-W chronology of core formation in planetesimals. Earth Planet. Sci. Lett. 361, 162-172.
Kurtz, A.C., Kump, L.R., Arthur, M.A., Zachos, J.C., Paytan, A., 2003. Early Cenozoic decoupling of the global carbon and sulfur cycles. Paleoceanography 18.

1469 Lauretta, D.S., Devouard, B., Buseck, P.R., 1999. The cosmochemical behavior of mercury. Earth Planet.
1470 Sci. Lett. 171, 35-47.
1471 Lauretta, D.S., Klaue, B., Blum, J.D., Buseck, P.R., 2001. Mercury abundances and isotopic compositions
1472 in the Murchison (CM) and Allende (CV) carbonaceous chondrites. Geochim. Cosmochim. Acta.
1473 65, 2807-2818.
1474 Lee, D.-C., Halliday, A.N., Hein, J.R., Burton, K.W., Christensen, J.N., Günther, D., 1999. Hafnium
1475 isotope stratigraphy of ferromanganese crusts. Science 285, 1052-1054.
1476 Lipschutz, M.E., Woolum, D.S., 1988. Highly labile elements, in: Kerridge, J.F., Matthews, M.S. (Eds.),
1477 Meteorites and the early solar system. Univerisity of Arizona Press, pp. 462-487.
1478 Lodders, K., 2003. Solar system abundances and condensation temperatures of the elements. Astrophys.
1479 J. 591, 1220-1247.
1480 Marschall, H.R., Pogge von Strandmann, P.A.E., Seitz, H.M., Elliott, T., Niu, Y.L., 2007. The lithium
1481 isotopic composition of orogenic eclogites and deep subducted slabs. Earth Planet. Sci. Lett. 262,
1482 563-580.
1483 Matthews, A.D., Riley, J.P., 1970. The occurrence of thallium in sea water and marine sediments. Chem.
1484 Geol. 149, 149-152.
1485 McDonough, W.F., Sun, S.-s., 1995. The composition of the Earth. Chem. Geol. 120, 223-253.
1486 McGoldrick, P.J., Keays, R.R., Scott, B.B., 1979. Thallium - Sensitive Indicator of Rock-Seawater
1487 Interaction and of Sulfur Saturation of Silicate Melts. Geochim. Cosmochim. Acta. 43, 1303-
1488 1311.
1489 Metz, S., Trefry, J.H., 2000. Chemical and mineralogical influences on concentrations of trace metals in
1490 hydrothermal fluids. Geochim. Cosmochim. Acta. 64, 2267-2279.
1491 Mottl, M.J., 2003. Partitioning of energy and mass fluxes between mid-ocean ridge axes and flanks at
1492 high and low temperature, in: Halbach, P.E., Tunnicliffe, V., Hein, J.R. (Eds.), Energy and mass
1493 transfer in marine hydrothermal systems. Dahlem University Press, pp. 271-286.
1494 Nielsen, S.G., 2010. Potassium and uranium in the upper mantle controlled by Archean oceanic crust
1495 recycling. Geology 38, 683-686.
1496 Nielsen, S.G., Goff, M., Hesselbo, S.P., Jenkyns, H.C., LaRowe, D.E., Lee, C.T.A., 2011. Thallium
1497 isotopes in early diagenetic pyrite – A paleoredox proxy? Geochim. Cosmochim. Acta. 75, 6690-
1498 6704.
1499 Nielsen, S.G., Klein, F., Kading, T., Blusztajn, J., Wickham, K., 2015. Thallium as a Tracer of Fluid-
1500 Rock Interaction in the Shallow Mariana Forearc. Earth Planet. Sci. Lett. 430, 416-426.
1501 Nielsen, S.G., Lee, C.T.A., 2013. Determination of thallium in the USGS glass reference materials BIR-
1502 1G, BHVO-2G and BCR-2G and application to quantitative Tl concentrations by LA-ICP-MS.
1503 Geostand. Geoanal. Res. 37, 337-343.
1504 Nielsen, S.G., Mar-Gerrison, S., Gannoun, A., LaRowe, D.E., Klemm, V., Halliday, A.N., Burton, K.W.,
1505 Hein, J.R., 2009a. Thallium Isotope Evidence for Increased Marine Organic Carbon Export in the
1506 Early Eocene. Earth Planet. Sci. Lett. 278, 297-307.
1507 Nielsen, S.G., Rehkämper, M., Baker, J., Halliday, A.N., 2004. The precise and accurate determination of
1508 thallium isotope compositions and concentrations for water samples by MC-ICPMS. Chem. Geol.
1509 204, 109-124.
1510 Nielsen, S.G., Rehkämper, M., Brandon, A.D., Norman, M.D., Turner, S., O'Reilly, S.Y., 2007. Thallium
1511 isotopes in Iceland and Azores lavas - Implications for the role of altered crust and mantle
1512 geochemistry. Earth Planet. Sci. Lett. 264, 332-345.
1513 Nielsen, S.G., Rehkämper, M., Halliday, A.N., 2006a. Large thallium isotopic variations in iron
1514 meteorites and evidence for lead-205 in the early solar system. Geochim. Cosmochim. Acta. 70,
1515 2643-2657.
1516 Nielsen, S.G., Rehkämper, M., Norman, M.D., Halliday, A.N., Harrison, D., 2006b. Thallium isotopic
1517 evidence for ferromanganese sediments in the mantle source of Hawaiian basalts. Nature 439,
1518 314-317.

1519 Nielsen, S.G., Rehkämper, M., Porcelli, D., Andersson, P., Halliday, A.N., Swarzenski, P.W., Latkoczy,
1520 C., Gunther, D., 2005a. Thallium isotope composition of the upper continental crust and rivers -
1521 An investigation of the continental sources of dissolved marine thallium. Geochim. Cosmochim.
1522 Acta. 69, 2007-2019.
1523 Nielsen, S.G., Rehkämper, M., Porcelli, D., Andersson, P.S., Halliday, A.N., Swarzenski, P.W., Latkoczy,
1524 C., Günther, D., 2005b. The thallium isotope composition of the upper continental crust and
1525 rivers - An investigation of the continental sources of dissolved marine thallium. Geochim.
1526 Cosmichim. Acta 69, 2007-2019.
1527 Nielsen, S.G., Rehkämper, M., Teagle, D.A.H., Alt, J.C., Butterfield, D., Halliday, A.N., 2006c.
1528 Hydrothermal fluid fluxes calculated from the isotopic mass balance of thallium in the ocean
1529 crust. Earth Planet. Sci. Lett. 251, 120-133.
1530 Nielsen, S.G., Shimizu, N., Lee, C.T.A., Behn, M., 2014. Chalcophile behavior of thallium during MORB
1531 melting and implications for the sulfur content of the mantle. Geochem. Geophys. Geosyst. 15,
1532 4905-4919.
1533 Nielsen, S.G., Wasylenki, L.E., Rehkämper, M., Peacock, C.L., Xue, Z., Moon, E.M., 2013. Towards an
1534 understanding of thallium isotope fractionation during adsorption to manganese oxides. Geochim.
1535 Cosmochim. Acta. 117, 252-265.
1536 Nielsen, S.G., Williams, H.M., Griffin, W.L., O'Reilly, S.Y., Pearson, N., Viljoen, K.S., 2009b. Thallium
1537 isotopes as a potential tracer for the origin of cratonic eclogites? Geochim. Cosmochim. Acta. 73,
1538 7387-7398.
1539 Nielsen, S.G., Yogodzinski, G.M., Prytulak, J., Plank, T., Kay, S.M., Kay, R.W., Blusztajn, J., Owens,
1540 J.D., Auro, M., Kading, T., 2016. Tracking along-arc sediment inputs to the Aleutian arc using
1541 thallium isotopes. Geochim. Cosmochim. Acta. 181, 217-237.
1542 Noll, P.D., Newsom, H.E., Leeman, W.P., Ryan, J.G., 1996. The role of hydrothermal fluids in the
1543 production of subduction zone magmas: Evidence from siderophile and chalcophile trace
1544 elements and boron. Geochim. Cosmochim. Acta. 60, 587-611.
1545 Nriagu, J., 1998. Thallium in the Environment, Advances in environental sciences and technology. Wiley,
1546 New York.
1547 Ostic, R.G., Elbadry, H.M., Kohman, T.P., 1969. Isotopic Composition of Meteoritic Thallium. Earth
1548 Planet. Sci. Lett. 7, 72-76.
1549 Owens, J.D., Nielsen, S.G., Peterson, L.C., Caffrey, P., 2016. Thallium isotope cycling in euxinic
1550 sediments. Geochim. Cosmochim. Acta. In prep.
1551 Palk, C.S., Rehkämper, M., Andreasen, R., Stunt, A., 2011. Extreme cadmium and thallium isotope
1552 fractionations in enstatite chondrites. Meteorit. Planet. Sci. 46, A183-A183.
1553 Patterson, C.C., Settle, D.M., 1987. Magnitude of Lead Flux to the Atmosphere from Volcanos. Geochim.
1554 Cosmochim. Acta. 51, 675-681.
1555 Paytan, A., Kastner, M., Campbell, D., Thiemens, M.H., 1998. Sulfur isotopic composition of Cenozoic
1556 seawater sulfate. Science 282, 1459-1462.
1557 Paytan, A., Kastner, M., Campbell, D., Thiemens, M.H., 2004. Seawater sulfur isotope fluctuations in the
1558 cretaceous. Science 304, 1663-1665.
1559 Peacock, C.L., Moon, E.M., 2012. Oxidative scavenging of thallium by birnessite: Controls on thallium
1560 sorption and stable isotope fractionation in marine ferromanganese precipitates. Geochim.
1561 Cosmochim. Acta. 84, 297-313.
1562 Pengra, J.G., Genz, H., Fink, R.W., 1978. Orbital electron capture ratios in the decay of ^{205}Pb. Nuclear
1563 Physics A302, 1-11.
1564 Peter, A.L.J., Viraraghavan, T., 2005. Thallium: a review of public health and environmental concerns.
1565 Environ Int 31, 493-501.
1566 Pietruszka, A.J., Reznik, A.D., 2008. Identification of a matrix effect in the MC-ICP-MS due to sample
1567 purification using ion exchange resin: An isotopic case study of molybdenum. Int. J. Mass
1568 Spectrom. 270, 23-30.

Pogge von Strandmann, P.A.E., Burton, K.W., James, R.H., van Calsteren, P., Gislason, S.R., 2010. Assessing the role of climate on uranium and lithium isotope behaviour in rivers draining a basaltic terrain. Chem. Geol. 270, 227-239.
Poirier, A., Doucelance, R., 2009. Effective Correction of Mass Bias for Rhenium Measurements by MC-ICP-MS. Geostand. Geoanal. Res. 33, 195-204.
Prytulak, J., Nielsen, S.G., Plank, T., Barker, M., Elliott, T., 2013. Assessing the utility of thallium and thallium isotopes for tracing subduction zone inputs to the Mariana arc. Chem. Geol. 345, 139-149.
Rehkämper, M., Frank, M., Hein, J.R., Halliday, A., 2004. Cenozoic marine geochemistry of thallium deduced from isotopic studies of ferromanganese crusts and pelagic sediments. Earth Planet. Sci. Lett. 219, 77-91.
Rehkämper, M., Frank, M., Hein, J.R., Porcelli, D., Halliday, A., Ingri, J., Liebetrau, V., 2002. Thallium isotope variations in seawater and hydrogenetic, diagenetic, and hydrothermal ferromanganese deposits. Earth Planet. Sci. Lett. 197, 65-81.
Rehkämper, M., Halliday, A.N., 1999. The precise measurement of Tl isotopic compositions by MC-ICPMS: Application to the analysis of geological materials and meteorites. Geochim. Cosmochim. Acta. 63, 935-944.
Rehkämper, M., Nielsen, S.G., 2004. The mass balance of dissolved thallium in the oceans. Mar. Chem. 85, 125-139.
Rehkämper, M., Wombacher, F., Horner, T.J., Xue, Z., 2012. Natural and Anthropogenic Cd Isotope Variations, in: Baskaran, M. (Ed.), Handbook of Environmental Isotope Geochemistry: Vol I. Springer Berlin Heidelberg, Berlin, Heidelberg, pp. 125-154.
Renne, P.R., 2000. Ar-40/Ar-39 age of plagioclase from Acapulco meteorite and the problem of systematic errors in cosmochronology. Earth Planet. Sci. Lett. 175, 13-26.
Ridley, W.I., Stetson, S.J., 2006. A review of isotopic composition as an indicator of the natural and anthropogenic behavior of mercury. Appl. Geochem. 21, 1889-1899.
Rosman, K.J.R., Chisholm, W., Boutron, C.F., Candelone, J.P., Patterson, C.C., 1994. Anthropogenic lead isotopes in Antarctica. Geophys. Res. Lett. 21, 2669-2672.
Rudge, J.F., Reynolds, B.C., Bourdon, B., 2009. The double spike toolbox. Chem. Geol. 265, 420-431.
Rudnick, R.L., Gao, S., 2003. Composition of the Continental Crust, in: Holland, H.D., Turekian, K.K. (Eds.), Treatise on Geochemistry. Pergamon, Oxford, pp. 1-64.
Salters, V.J.M., Stracke, A., 2004. Composition of the depleted mantle. Geochem. Geophys. Geosyst. 5.
Sawlan, J.J., Murray, J.W., 1983. Trace-metal Remobilisation in the Interstitial Waters of red Clay and Hemipelagic Marine Sediments. Earth Planet. Sci. Lett. 64, 213-230.
Schauble, E.A., 2007. Role of nuclear volume in driving equilibrium stable isotope fractionation of mercury, thallium, and other very heavy elements. Geochim. Cosmochim. Acta. 71, 2170-2189.
Schedlbauer, O.F., Heumann, K.G., 2000. Biomethylation of Thallium by Bacteria and First Determination of Biogenic Dimethylthallium in the Ocean. Appl. Organometal. Chem. 14, 330-340.
Schönbächler, M., Carlson, R.W., Horan, M.F., Mock, T.D., Hauri, E.H., 2008. Silver isotope variations in chondrites: Volatile depletion and the initial Pd-107 abundance of the solar system. Geochim. Cosmochim. Acta. 72, 5330-5341.
Segl, M., Mangini, A., Beer, J., Bonani, G., Suter, M., Wolfli, W., 1989. Growth rate variations of manganese nodules and crusts induced by paleoceanographic events. Paleoceanography 4, 511-530.
Segl, M., Mangini, A., Bonani, G., Hofmann, H.J., Nessi, M., Suter, M., Wolfli, W., Friedrich, G., Pluger, W.L., Wiechowski, A., Beer, J., 1984. Be-10-Dating of a Manganese Crust from Central North Pacific and Implications for Ocean Palaeocirculation. Nature 309, 540-543.
Settle, D.M., Patterson, C.C., 1982. Magnitudes and Sources of Precipitation and Dry Deposition Fluxes of Industrial and Natural Leads to the North Pacific at Enewetak. Journal of Geophysical Research-Oceans and Atmospheres 87, 8857-8869.

Shannon, R.D., 1976. Revised effective ionic radii and systematic studies of interatomic distances in halides and chalcogenides. Acta Crystallographica A32, 751-767.
Shaw, D.M., 1952. The geochemistry of thallium. Geochim. Cosmochim. Acta. 2, 118-154.
Shiel, A.E., Barling, J., Orians, K.J., Weis, D., 2009. Matrix effects on the multi-collector inductively coupled plasma mass spectrometric analysis of high-precision cadmium and zinc isotope ratios. Analytica Chimica Acta 633, 29-37.
Shukolyukov, A., Lugmair, G.W., 2006. Manganese-chromium isotope systematics of carbonaceous chondrites. Earth Planet. Sci. Lett. 250, 200-213.
Sprung, P., Scherer, E.E., Upadhyay, D., Leya, I., Mezger, K., 2010. Non-nucleosynthetic heterogeneity in non-radiogenic stable Hf isotopes: Implications for early solar system chronology. Earth Planet. Sci. Lett. 295, 1-11.
Sugiura, N., Hoshino, H., 2003. Mn-Cr chronology of five IIIAB iron meteorites. Meteorit. Planet. Sci. 38, 117-143.
Teagle, D.A.H., Alt, J.C., Bach, W., Halliday, A.N., Erzinger, J., 1996. Alteration of upper ocean crust in a ridge-flank hydrothermal upflow zone: Mineral, chemical, and isotopic constraints from hole 896A. Proc. ODP Sci. Results 148, 119-150.
Theis, K.J., Schönbächler, M., Benedix, G.K., Rehkämper, M., Andreasen, R., Davies, C., 2013. Palladium-silver chronology of IAB iron meteorites. Earth Planet. Sci. Lett. 361, 402-411.
Thirlwall, M.F., Gee, M.A.M., Taylor, R.N., Murton, B.J., 2004. Mantle components in Iceland and adjacent ridges investigated using double-spike Pb isotope ratios. Geochim. Cosmochim. Acta. 68, 361-386.
Trieloff, M., Jessberger, E.K., Herrwerth, I., Hopp, J., Fieni, C., Ghelis, M., Bourot-Denise, M., Pellas, P., 2003. Structure and thermal history of the H-chondrite parent asteroid revealed by thermochronometry. Nature 422, 502-506.
Tsuchiyama, A., Kawamura, K., Nakao, T., Uyeda, C., 1994. Isotopic effects on diffusion in MgO melt simulated by the molecular-dynamics (Md) method and implications for isotopic mass fractionation in magmatic systems. Geochim. Cosmochim. Acta. 58, 3013-3021.
Turner, A., Cabon, A., Glegg, G.A., Fisher, A.S., 2010. Sediment-water interactions of thallium under simulated estuarine conditions. Geochim. Cosmochim. Acta. 74, 6779-6787.
Urey, H.C., 1947. The thermodynamic properties of isotopic substances. J. Chem. Soc., 562-581.
van de Flierdt, T., Frank, M., Halliday, A.N., Hein, J.R., Hattendorf, B., Gunther, D., Kubik, P.W., 2004. Tracing the history of submarine hydrothermal inputs and the significance of hydrothermal hafnium for the seawater budget-a combined Pb-Hf-Nd isotope approach. Earth Planet. Sci. Lett. 222, 259-273.
Vogel, N., Renne, P.R., 2008. Ar-40-Ar-39 dating of plagioclase grain size separates from silicate inclusions in IAB iron meteorites and implications for the thermochronological evolution of the IAB parent body. Geochim. Cosmochim. Acta. 72, 1231-1255.
Walker, R.J., 2012. Evidence for homogeneous distribution of osmium in the protosolar nebula. Earth Planet. Sci. Lett. 351, 36-44.
Wallmann, K., 2001. Controls on the Cretaceous and Cenozoic evolution of seawater composition, atmospheric CO2 and climate. Geochim. Cosmochim. Acta. 65, 3005-3025.
Wasserburg, G.J., Busso, M., Gallino, R., Nollett, K.M., 2006. Short-lived nuclei in the early Solar System: Possible AGB sources. Nucl Phys A 777, 5-69.
Wasserburg, G.J., Busso, M., Gallino, R., Raiteri, C.M., 1994. Asymptotic giant branch stars as a source of short-lived radioactive nuclei in the solar nebula. Astrophys. J. 424, 412-428.
Wedepohl, K.H., 1974. Handbook of Geochemistry. Springer.
Wedepohl, K.H., 1995. The composition of the continental crust. Geochim. Cosmochim. Acta. 59, 1217-1232.
Williams, H., Turner, S., Kelley, S., Harris, N., 2001. Age and composition of dikes in Southern Tibet: New constraints on the timing of east-west extension and its relationship to postcollisional volcanism. Geology 29, 339-342.

Williams, H.M., McCammon, C.A., Peslier, A.H., Halliday, A.N., Teutsch, N., Levasseur, S., Burg, J.P., 2004. Iron isotope fractionation and the oxygen fugacity of the mantle. Science 304, 1656-1659.

Williams, H.M., Nielsen, S.G., Renac, C., Griffin, W.L., O'Reilly, S.Y., McCammon, C., Pearson, N., 2009. Fractionation of oxygen and iron isotopes in the mantle: implications for crustal recycling and the source regions of oceanic basalts. Earth Planet. Sci. Lett. 283, 156-166.

Wombacher, F., Rehkämper, M., Mezger, K., Bischoff, A., Münker, C., 2008. Cadmium stable isotope cosmochemistry. Geochim. Cosmochim. Acta. 72, 646-667.

Wombacher, F., Rehkämper, M., Mezger, K., Münker, C., 2003. Stable isotope compositions of cadmium in geological materials and meteorites determined by multiple-collector ICPMS. Geochim. Cosmochim. Acta. 67, 4639-4654.

Wood, B.J., Nielsen, S.G., Rehkämper, M., Halliday, A.N., 2008. The effects of core formation on the Pb- and Tl- isotopic composition of the silicate Earth. Earth Planet. Sci. Lett. 269, 325-335.

Woodland, S.J., Rehkämper, M., Halliday, A., Lee, D.-C., Hattendorf, B., Günther, D., 2005. Accurate measurement of silver isotope composition in geological materials including low Pd/Ag meteorites. Geochim. Cosmochim. Acta. 69, 2153-2163.

Xiao, T.F., Boyle, D., Guha, J., Rouleau, A., Hong, Y.T., Zheng, B.S., 2003. Groundwater-related thallium transfer processes and their impacts on the ecosystem: southwest Guizhou Province, China. Appl. Geochem. 18, 675-691.

Xiao, T.F., Guha, J., Boyle, D., Liu, C.Q., Chen, J.G., 2004. Environmental concerns related to high thallium levels in soils and thallium uptake by plants in southwest Guizhou, China. Sci. Total Environ. 318, 223-244.

Xiao, T.F., Guha, J., Liu, C.Q., Zheng, B.S., Wilson, G., Ning, Z.P., He, L.B., 2007. Potential health risk in areas of high natural concentrations of thallium and importance of urine screening. Appl. Geochem. 22, 919-929.

Xiong, Y.L., 2007. Hydrothermal thallium mineralization up to 300 degrees C: A thermodynamic approach. Ore Geol Rev 32, 291-313.

Yokoi, K., Takahashi, K., Arnould, M., 1985. The Production and Survival of Pb-205 in Stars, and the Pb-205- Tl-205 S-Process Chronometry. Astron. Astrophys. 145, 339-346.

Yokoyama, T., Rai, V.K., Alexander, M.O., Lewis, R.S., Carlson, R.W., Shirey, S.B., ThiernenS, M.H., Walker, R.J., 2007. Osmium isotope evidence for uniform distribution of s- and r-process components in the early solar system. Earth Planet. Sci. Lett. 259, 567-580.

1707 Table 1: Physical properties of thallium (Nriagu, 1998)

Melting point	577 K
Molar weight	204.38 g
Density	11.85 g/cm^3
Valence states	Tl^0 Tl^+ Tl^{3+}
Redox potentials (V)	
$Tl_{(s)} \rightarrow Tl^+ + e^-$	+0.336
$Tl^+ \rightarrow Tl^{3+} + 2e^-$	-1.28
Ionic radius (Tl^+)	1.50 Å
Ionic radius (Tl^{3+})	0.89 Å
Stable isotopes	^{203}Tl ^{205}Tl

1708

1709

Table 2: Tl isotope and concentration data for geologic reference materials

Standard	Description	ε^{205}Tl	n	Error[a]	Tl conc (ng/g)	Reference
Nod P1	USGS Ferromanganese nodule	0.5	1	0.5	146000	1
Nod A1[b]	USGS Ferromanganese nodule	10.7	6	0.5	108000	1,2
AGV-2	USGS Andesite	-3.0	8	0.6	269	3,4
BCR-2	USGS Columbia River basalt	-2.5	4	0.4	257	3
BHVO-1	USGS Hawaii Basalt	-3.5	10	0.5	37	3,8
BHVO-2	USGS Hawaii Basalt	-1.8	17	0.3	18	3,4,7
BIR-1	USGS Iceland basalt	1.1	6	1.2	1.3	5
NASS-5	Atlantic surface seawater	-5.0	1	1.0	0.0094	2
Allende	Carbonaceous chondrite	-3.1	8	0.5	55	6
BHVO-2G	USGS Basaltic glass	nd			16	9
BCR-2G	USGS Basaltic glass	nd			234	9
BIR-1G	USGS Basaltic glass	nd			2.5	9

References 1: (Rehkämper et al., 2002); 2: (Nielsen et al., 2004); 3:(Prytulak et al., 2013); 4: (Baker et al., 2009); 5: (Nielsen et al., 2007); 6: (Baker et al., 2010b); 7: (Coggon et al., 2014); 8: (Nielsen et al., 2015); 9: (Nielsen and Lee, 2013)

[a] – errors are either 2sd of the population of separate sample splits processed individually ($n \geq 3$) or estimated based on repeat measurements of similar samples ($n=1$).

[b] – Isotope composition reported for multiple analyses of one large 300mg aliquot dissolved in 6M HCl.

nd - not determined

1720 Table 3: Thallium isotope and concentration data for rivers

Sample	$\varepsilon^{205}Tl_{diss}$	Tl_{diss} (ng/kg)	$\varepsilon^{205}Tl_{part}$	Tl_{part} (ng/kg)
Amazon	-2.3	16.4		
Danube	-6.7	16.4	-2.9	3.6
Doubs	-5.5	3.36		
Eder	-4.2	1.93		
Kalix	-1.6	1.31	-3.8	0.29
Nahe	-2.5	7.03	-1.2	3.7
Nidda	-2.7	1.67		
Nidder	-2.6	2.85	-1.6	0.26
Nile	0.0	3.13		
Rhine Rueun	-6.4	3.61		
Rhine Laufenbg.	-3.0	4.04		
Rhine Speyer	-2.8	5.35		
Rhine Bingen	-2.9	6.71	-2.1	1.3
Rhone	-2.7	6.54	-2.2	36
Volga	-1.1	1.60		

1721 Uncertainty on Tl isotope measurements is ±1 ε^{205}Tl-unit

1722 Exact sample locations are given in Nielsen et al. (2005b)

1723

1724 Table 4: The Tl mass balance of the oceans with estimated source and sink fluxes.

	Range of Tl flux estimates (Mg/a)	Best estimate (Mg/a)		ε^{205}Tl	Ref.
Marine Input Fluxes					
Rivers	76 – 380	230	23%	-2.5	1, 2
Hydrothermal fluids	110 – 230	170	17%	-2	3, 9
Subaerial volcanism	42 – 700	370	37%	-2	6
Mineral aerosols	10 – 150	50	5%	-2	1, 2
Benthic fluxes from continental margins	5 – 390	170	17%	0	1, 7
Total Input Flux	465 – 1850	990	100%	-1.8	
Marine Output Fluxes					
Pelagic clays	240 – 450	310	36%	+10	1, 4, 7
Altered ocean crust	225 – 1985	680	64%	-7.2	1, 3, 7
Total Output Flux	465 –1850	940	100%	-1.8	

	Mass of Tl (Mg)	Steady-state residence time	ε^{205}Tl	
Global Oceans	1.75 (±0.14) x 10^7*	18,500 a	-6.0	1, 3, 5, 8

1725 References 1: (Rehkämper and Nielsen, 2004); 2: (Nielsen et al., 2005b); 3: (Nielsen et al.,
1726 2006c); 4: (Rehkämper et al., 2004); 5: (Rehkämper et al., 2002); 6: (Baker et al., 2009); 7: This
1727 study; 8: (Owens et al., 2016); 9: This work.
1728 * For a global ocean system with 1.348 x 10^{21} kg, the Tl mass in the oceans is equivalent to an
1729 average seawater concentration of 65±5 pmol/kg or 13±1 ng/kg (Rehkämper and Nielsen, 2004).
1730

FIGURE CAPTIONS:

Figure 1: Thallium isotope compositions and concentrations for terrestrial reservoirs relevant to subduction zones and recycled oceanic crust. Note the logarithmic scale for the concentrations. Data sourced from (Nielsen, 2010; Nielsen et al., 2015; Nielsen et al., 2006b; Nielsen et al., 2005a; Nielsen et al., 2006c; Nielsen et al., 2014; Nielsen et al., 2016; Prytulak et al., 2013; Rehkämper et al., 2004; Rehkämper et al., 2002).

Figure 2: Anion exchange separation procedures for Tl. The recipes can be scaled to any amount of resin (RV – resin volume) depending on sample size, though large samples require a second 100µl resin column to ensure that Tl is sufficiently pure. Four different elution procedures are outlined, as published by Baker et al., Nielsen et al. and Rehkämper and Halliday (2009; 2004; 1999).

Fig. 3. Pb–Tl isochron diagram for carbonaceous chondrites (modified from Baker et al., 2010b). Excluded from the plot and isochron calculation are two meteorites that exhibit stable Cd isotope fractionations as well as a sample of Allende Smithsonian due to contamination with terrestrial Pb (Baker et al., 2010b). All error bars are 2sd.

Fig. 4. Pb–Tl isochron diagrams for metal samples (filled symbols) and sulfides (open symbols) of IAB complex iron meteorites, based on the results of Nielsen et al. (2006a). The metal samples of Toluca and Canyon Diablo (CD) delineate a well-defined isochron. The isochron slope is slightly revised from Nielsen et al. (2006a), due to improved corrections for terrestrial Pb. The troilite nodules of these meteorites and metal and sulfide from the anomalous

IAB iron Mundrabilla do not plot on the IAB main group isochron defined by Toluca and Canyon Diablo, presumably due to stable isotope fractionation of Tl. All error bars are 2sd.

Fig. 5. Pb–Tl isochron diagram for metal samples of IIAB (squares) and IIIAB (diamonds) iron meteorites. The large and small symbols, with 2sd error bars, denote the data of Andreasen et al. (2012) and Nielsen et al. (2006a), respectively. The open diamond is for a troilite nodule of Grant IIIAB. Despite of the scatter and some large uncertainties, the results for both groups of magmatic irons display a positive correlation, which is indicative of radiogenic variations in Tl isotope composition from in situ decay of ^{205}Pb. The two errorchron trendlines were calculated from the data of Andreasen et al. (2012) only and correspond to initial $^{205}Pb/^{204}Pb_0$ ratios of $(8\pm2)\times10^{-4}$ and $(8\pm4)\times10^{-4}$ for the IIABs and the IIIABs, respectively.

Figure 6: Plot of $\varepsilon^{205}Tl$ vs. 1/total Tl concentration for soil samples from the vicinity of the Lengerich cement plant in Germany (modified from Kersten et al., 2014). Furthermore shown are results for a pyrite from the Meggen deposit (which is also the ultimate origin of the Tl-rich additive that was used in cement production) and the cement kiln dust (CKD). The linear trend and associated correlation coefficient R^2 were calculated from the soil data only. All error bars are 2sd.

Figure 7: Plots of (a) Ce/Tl and (b) Tl isotopes against depth for different sections of hydrothermally altered oceanic crust. Data compiled from (Coggon et al., 2014; Nielsen et al., 2006c; Prytulak et al., 2013; Teagle et al., 1996). The samples with error bars from ODP 801C

1776 are composites prepared from the lithologies encountered in these depth intervals (Kelley et al.,
1777 2003).
1778
1779 Figure 8: Thallium isotope compositions determined for the growth surfaces of hydrogenetic
1780 Fe-Mn crusts and seawater. The Fe-Mn crusts precipitate directly from seawater and hence there
1781 is an isotope fractionation of ~19 ε^{205}Tl-units (labeled α_{EMP}) between these two reservoirs. Data
1782 from (Nielsen et al., 2004; Nielsen et al., 2006c; Owens et al., 2016; Rehkämper et al., 2002).
1783 Also shown are the isotope fractionation factors (α_{EXP}) determined for experiments in which the
1784 manganese oxide birnessite was equilibrated with an aqueous Tl solution (Nielsen et al., 2013).
1785
1786 Figure 9: The S and Tl isotope composition of seawater over the last 75Myrs. The Tl isotope
1787 curve is based on a Fe-Mn crust from the Pacific Ocean and an inferred constant isotope
1788 fractionation factor of $\alpha = 1.0019$. The S isotope data are from Paytan et al. (1998, 2004), with
1789 ages based on the age model of Kurtz et al. (2003). The chronology of the Tl isotope curve was
1790 determined based on Os isotope data (Burton, 2006). Figure modified from Nielsen et al.
1791 (2009a).
1792
1793 Figure 10: Cs/Tl and Ce/Tl ratios of primitive basalts from Hawaii (Nielsen et al., 2006b)
1794 and Iceland (Nielsen et al., 2007) plotted versus Tl isotope composition. Mixing lines between
1795 pristine mantle (large pink square), Fe-Mn oxyhydroxides (blue squares) and low-T altered
1796 MORB (light green circles) are also shown. The mantle is assumed to be characterized by ε^{205}Tl
1797 = -2 (Nielsen et al., 2006b) and Ce, Cs and Tl concentrations of 772 ng/g, 4.2 ng/g and 0.7 ng/g,
1798 respectively (Nielsen et al., 2014; Salters and Stracke, 2004). For the Fe-Mn oxyhydroxides, the

1799 Tl concentration and isotope composition are assumed to be 100 µg/g and $\varepsilon^{205}Tl = +10$, akin to
1800 values of modern Fe-Mn crusts and nodules (Hein et al., 2000; Rehkämper et al., 2002). The Cs
1801 content of Fe-Mn oxyhydroxides is about 500 ng/g (Ben Othmann et al., 1989). Altered MORB
1802 is assumed to be characterized by $\varepsilon^{205}Tl = -10$ and Ce, Tl and Cs concentrations of about
1803 13400ng/g, 200ng/g and 200ng/g, respectively (Gale et al., 2013; Nielsen et al., 2006c). Error
1804 bars denote 2sd uncertainties.
1805

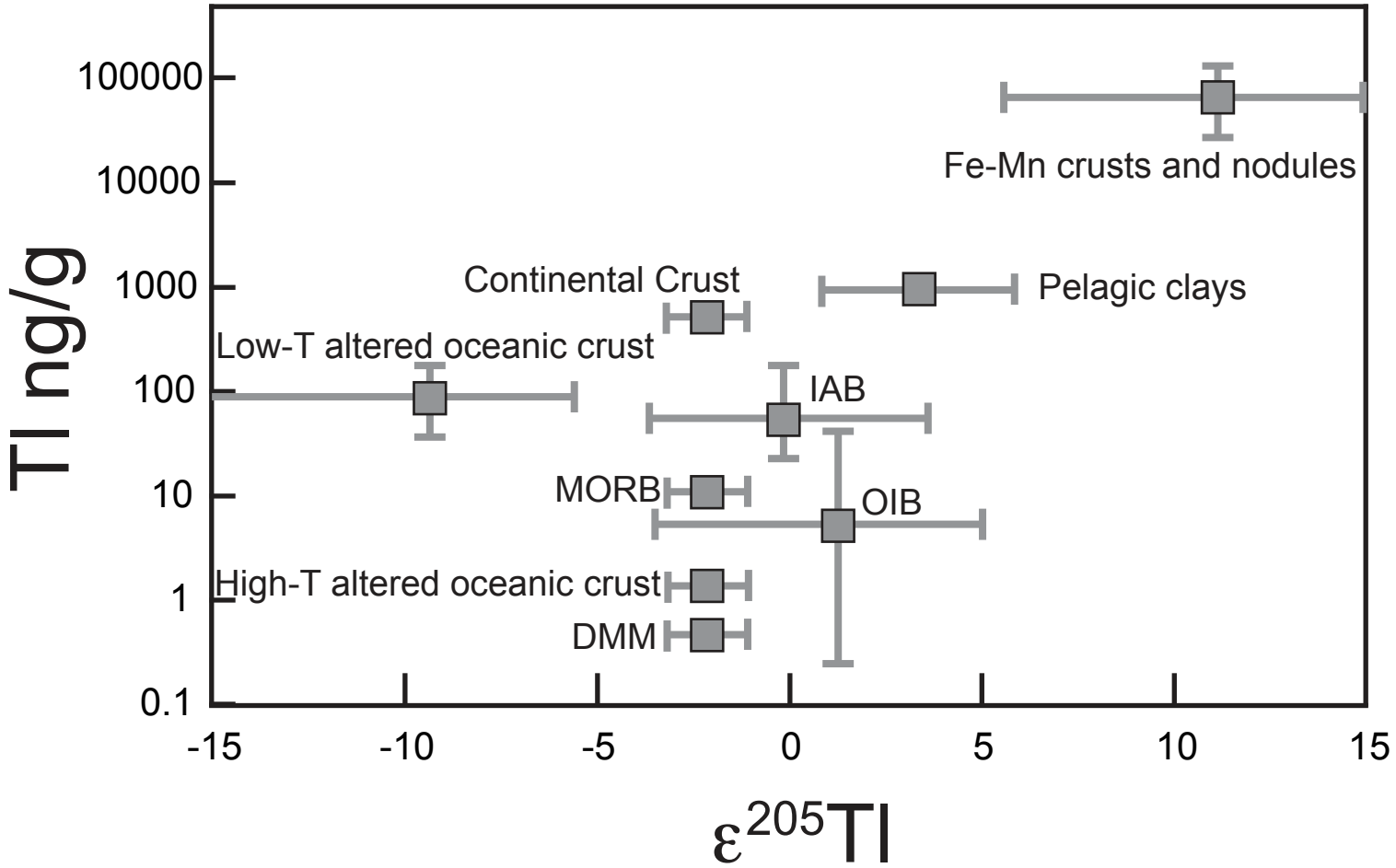
Tl ng/g
100000
10000
1000
100
10
1
0.1
-15
-10
-5
0
5
10
15
ε205Tl
Fe-Mn crusts and nodules
Continental Crust
Pelagic clays
Low-T altered oceanic crust
IAB
MORB
OIB
High-T altered oceanic crust
DMM

Tl chemistry; RV - resin volume

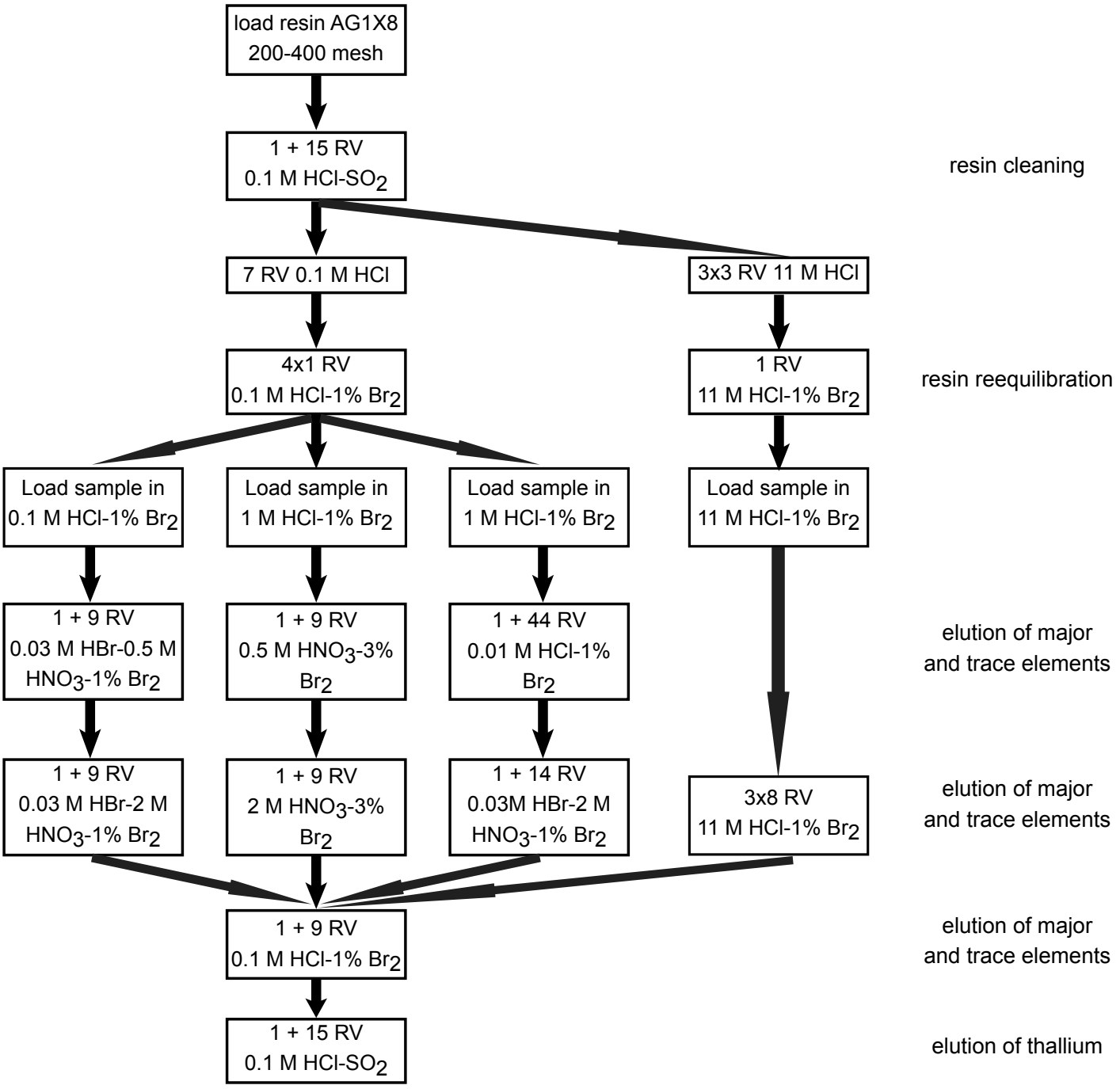

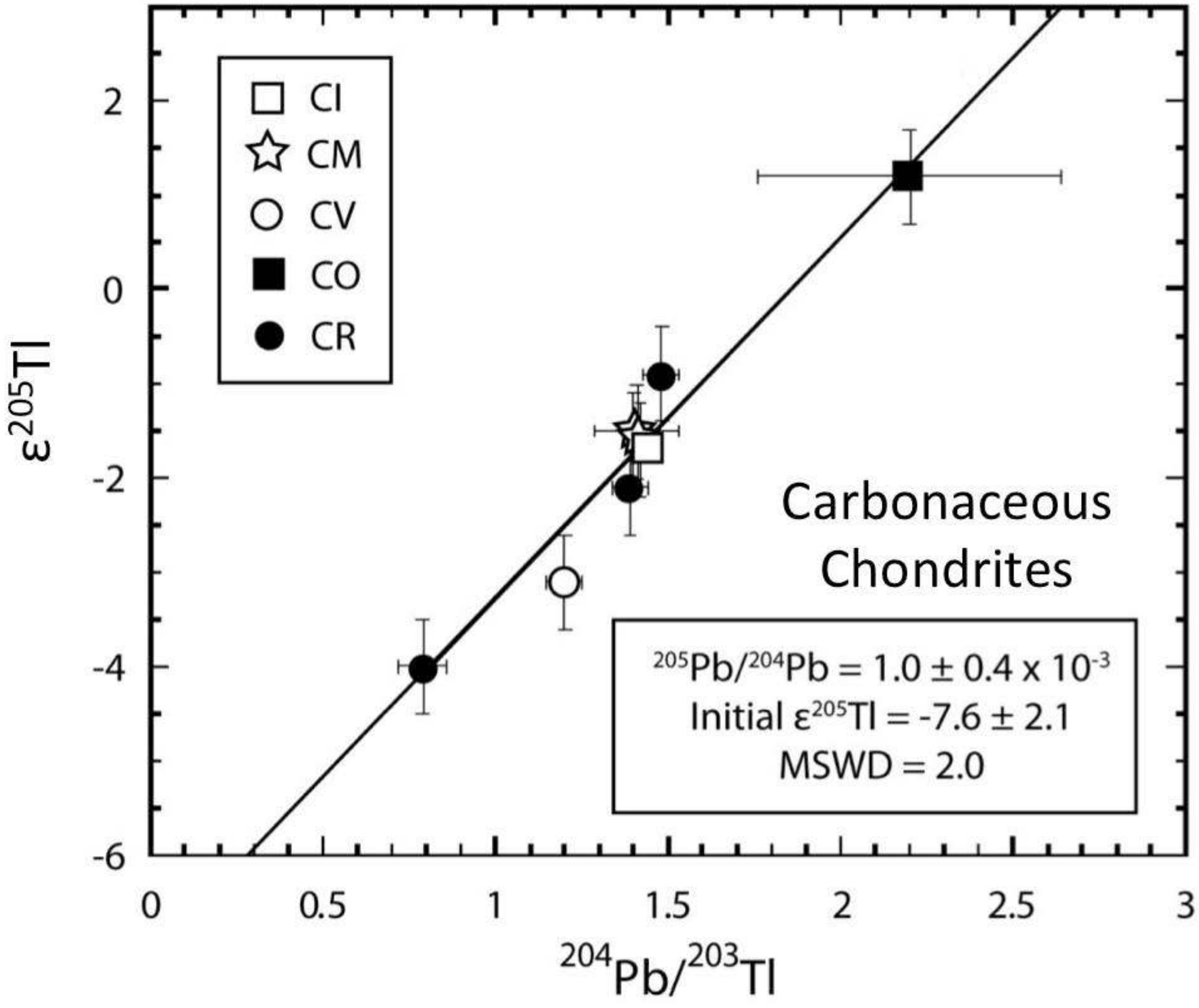
CI
CM
CV
CO
CR
Carbonaceous Chondrites
^{205}Pb/^{204}Pb = 1.0 ± 0.4 x 10^{-3}
Initial ε^{205}Tl = -7.6 ± 2.1
MSWD = 2.0
ε^{205}Tl
^{204}Pb/^{203}Tl
2
0
-2
-4
-6
0
0.5
1
1.5
2
2.5
3

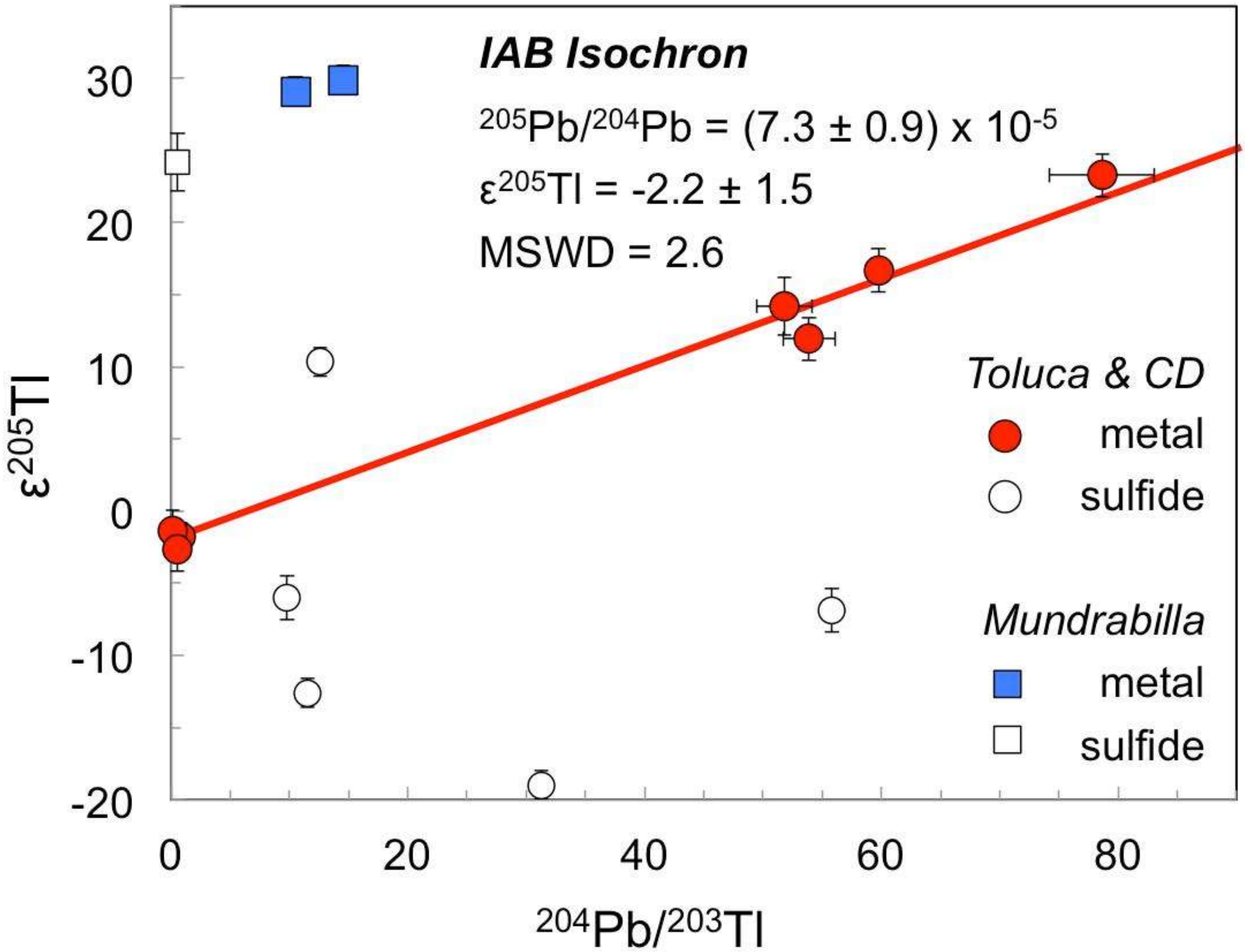
IAB Isochron
$^{205}Pb/^{204}Pb = (7.3 \pm 0.9) \times 10^{-5}$
$\varepsilon^{205}Tl = -2.2 \pm 1.5$
MSWD = 2.6
Toluca & CD
metal
sulfide
Mundrabilla
metal
sulfide
$\varepsilon^{205}Tl$
$^{204}Pb/^{203}Tl$
30
20
10
0
-10
-20
0
20
40
60
80

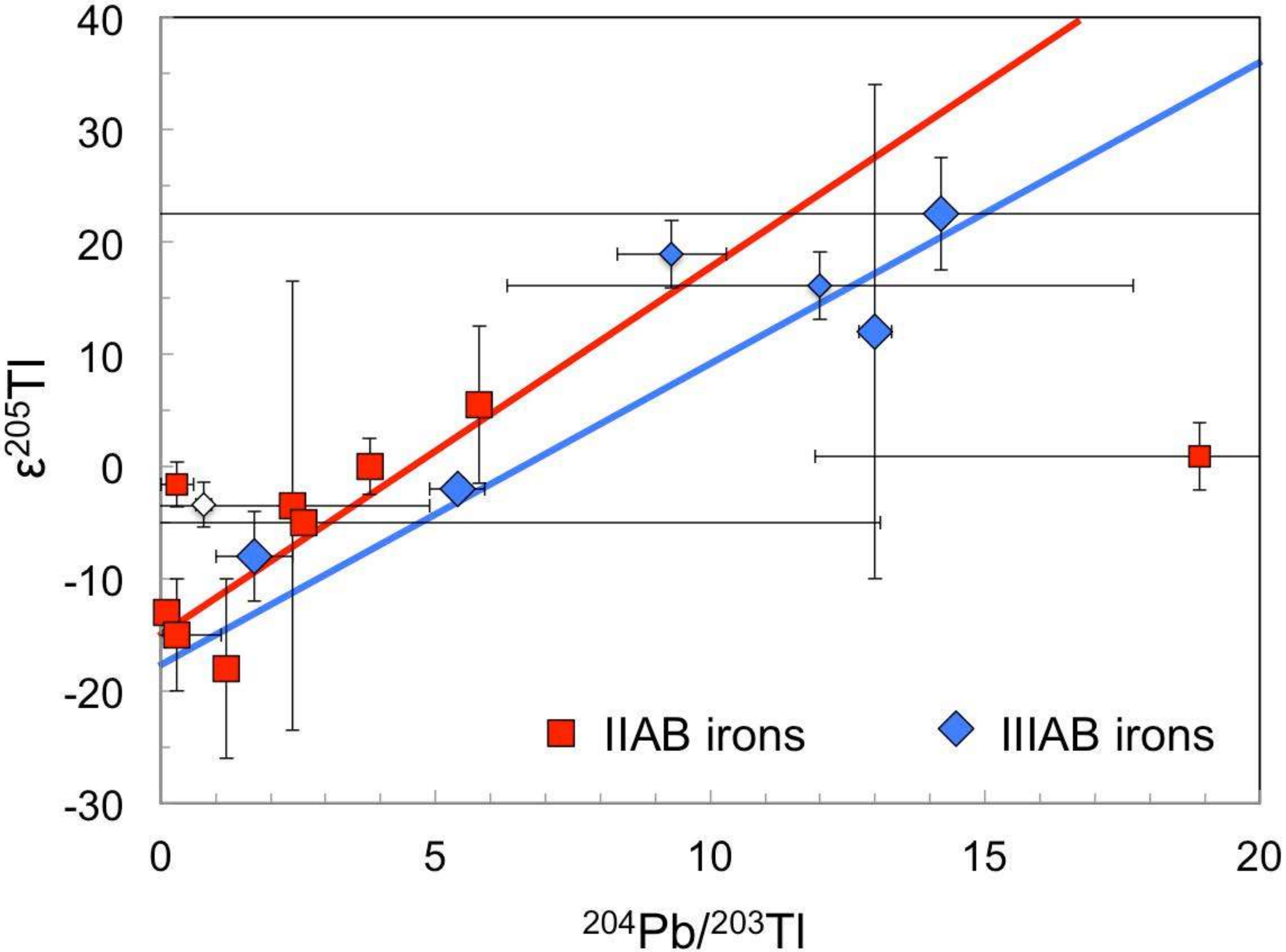
40
30
20
10
0
-10
-20
-30
0
5
10
15
20
ε^{205}Tl
^{204}Pb/^{203}Tl
IIAB irons
IIIAB irons

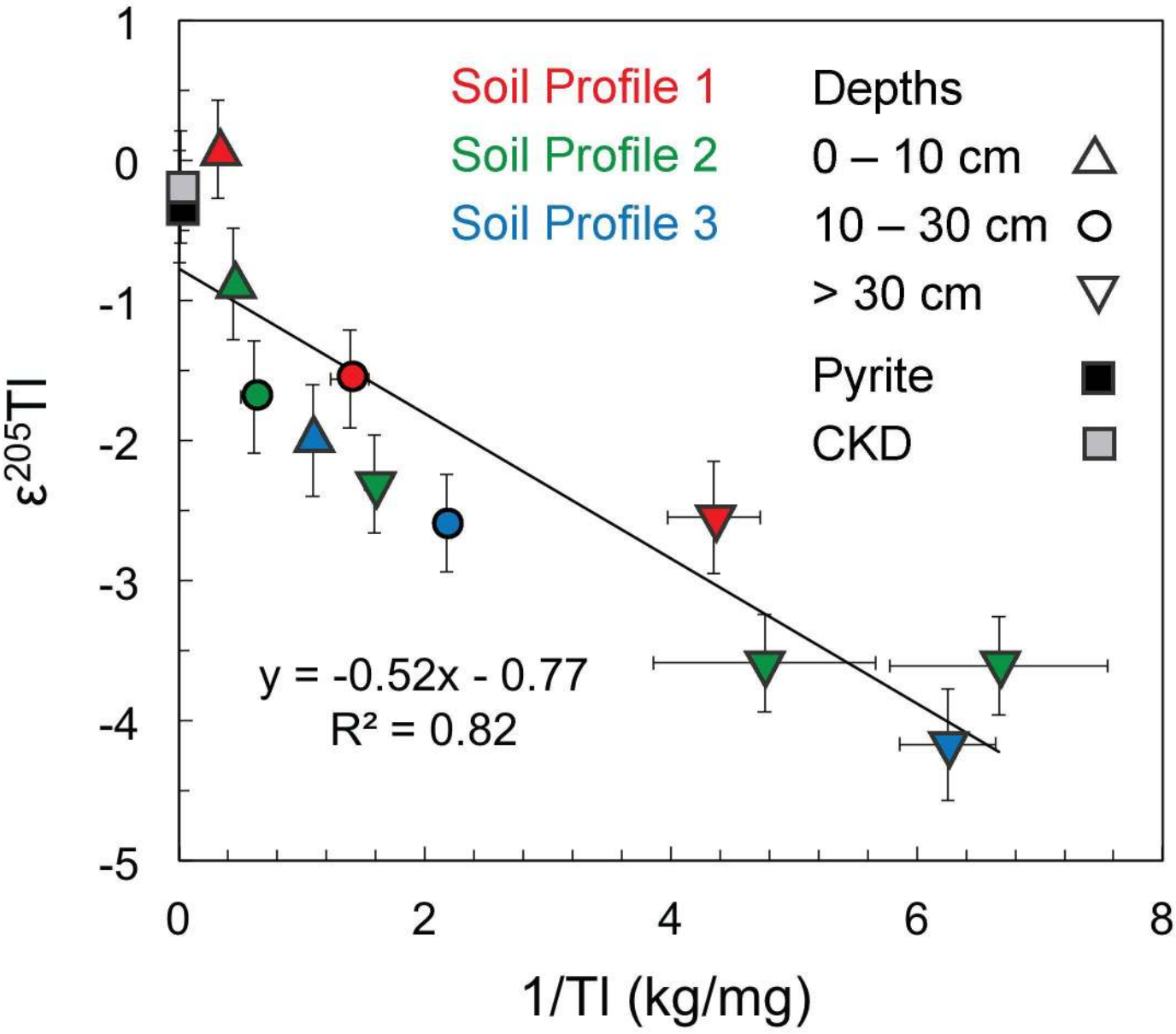
Soil Profile 1
Soil Profile 2
Soil Profile 3
Depths
0 – 10 cm
10 – 30 cm
> 30 cm
Pyrite
CKD
y = -0.52x - 0.77
R² = 0.82
ε205Tl
1/Tl (kg/mg)
1
0
-1
-2
-3
-4
-5
0
2
4
6
8

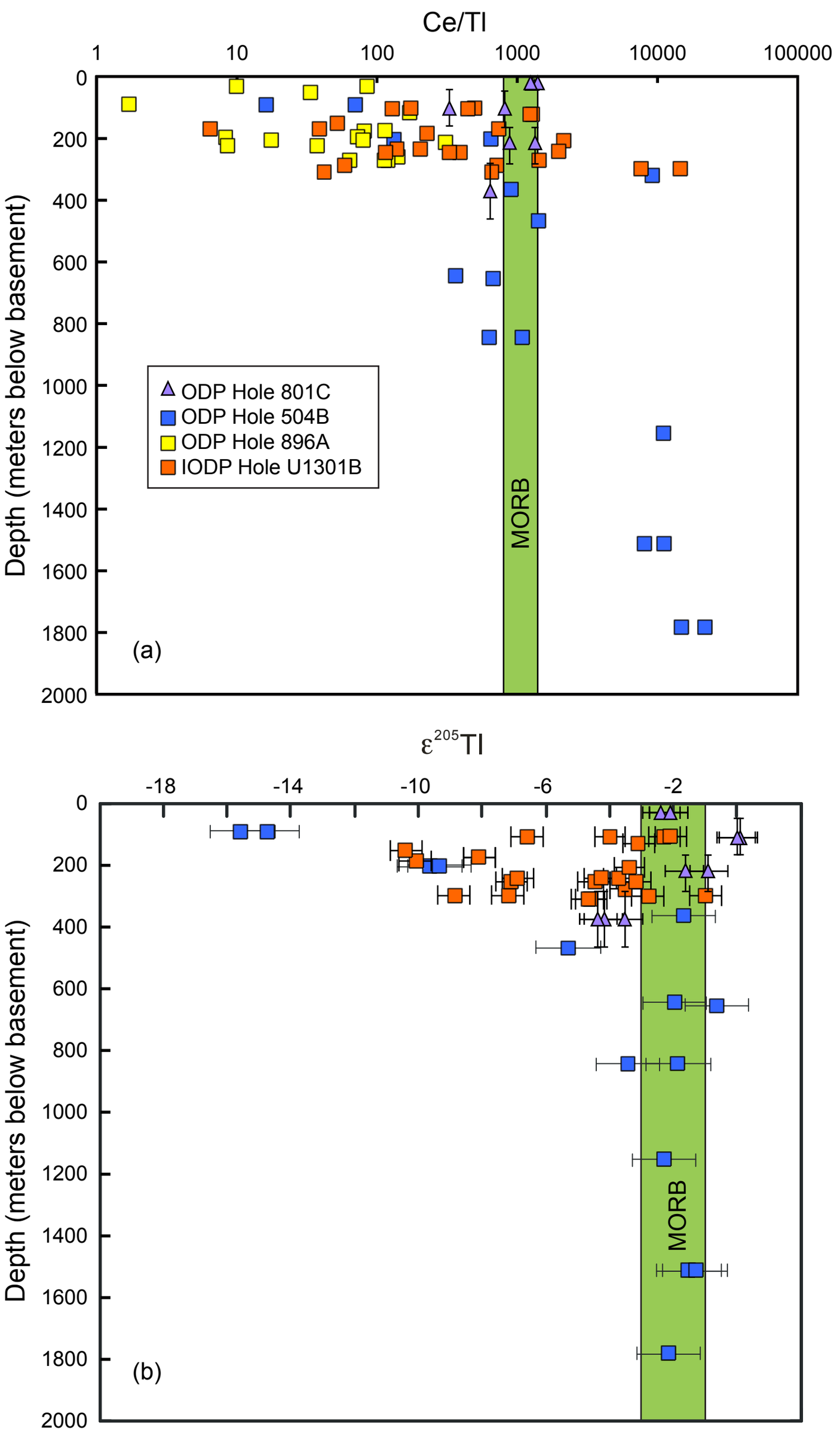
Ce/Tl
1
10
100
1000
10000
100000
0
200
400
600
800
1000
1200
1400
1600
1800
2000
Depth (meters below basement)
ODP Hole 801C
ODP Hole 504B
ODP Hole 896A
IODP Hole U1301B
MORB
(a)
ε205Tl
-18
-14
-10
-6
-2
0
200
400
600
800
1000
1200
1400
1600
1800
2000
Depth (meters below basement)
MORB
(b)

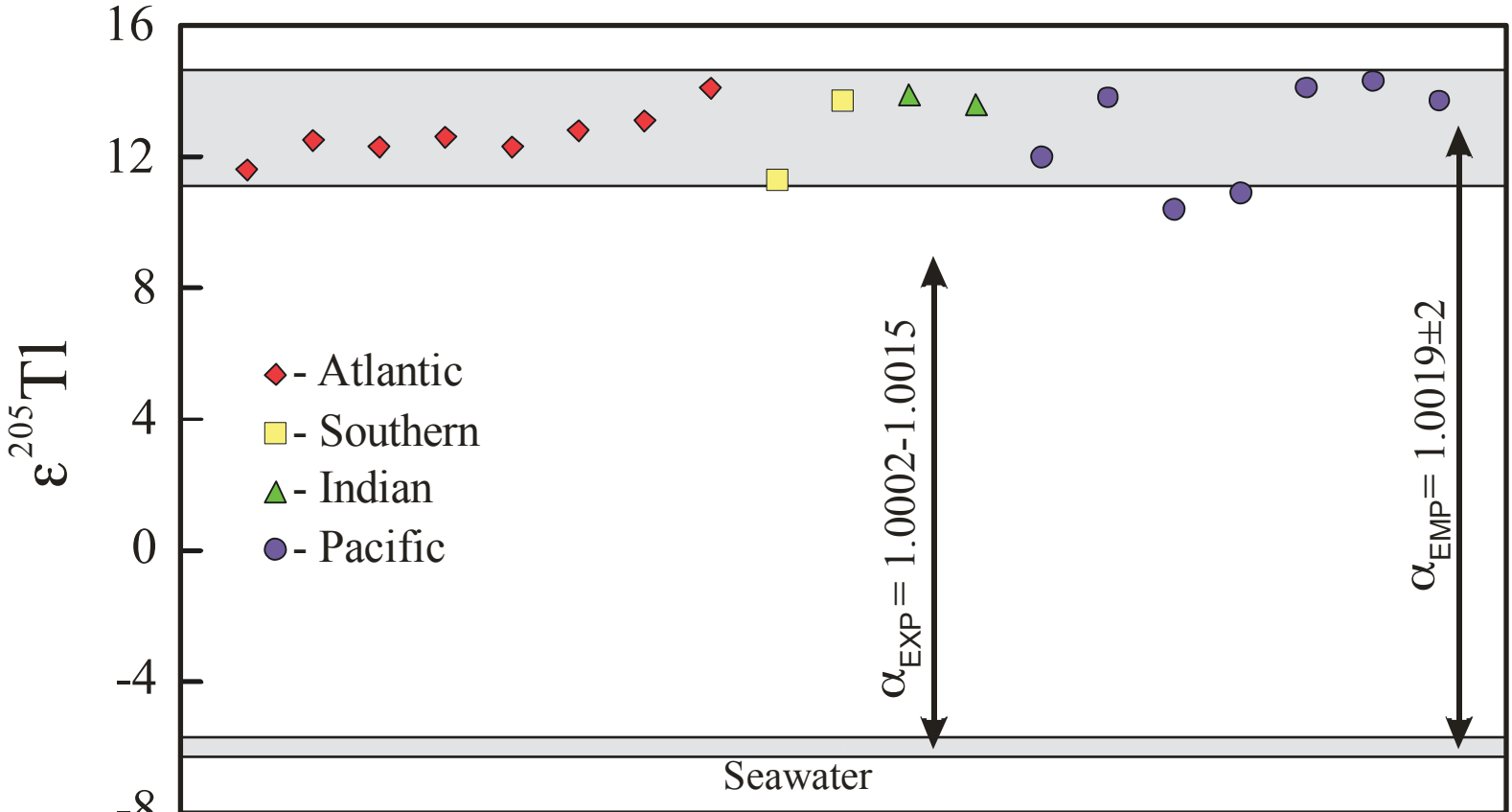
16
12
8
4
0
-4
-8
ε205Tl
- Atlantic
- Southern
- Indian
- Pacific
αEXP = 1.0002-1.0015
αEMP = 1.0019±2
Seawater

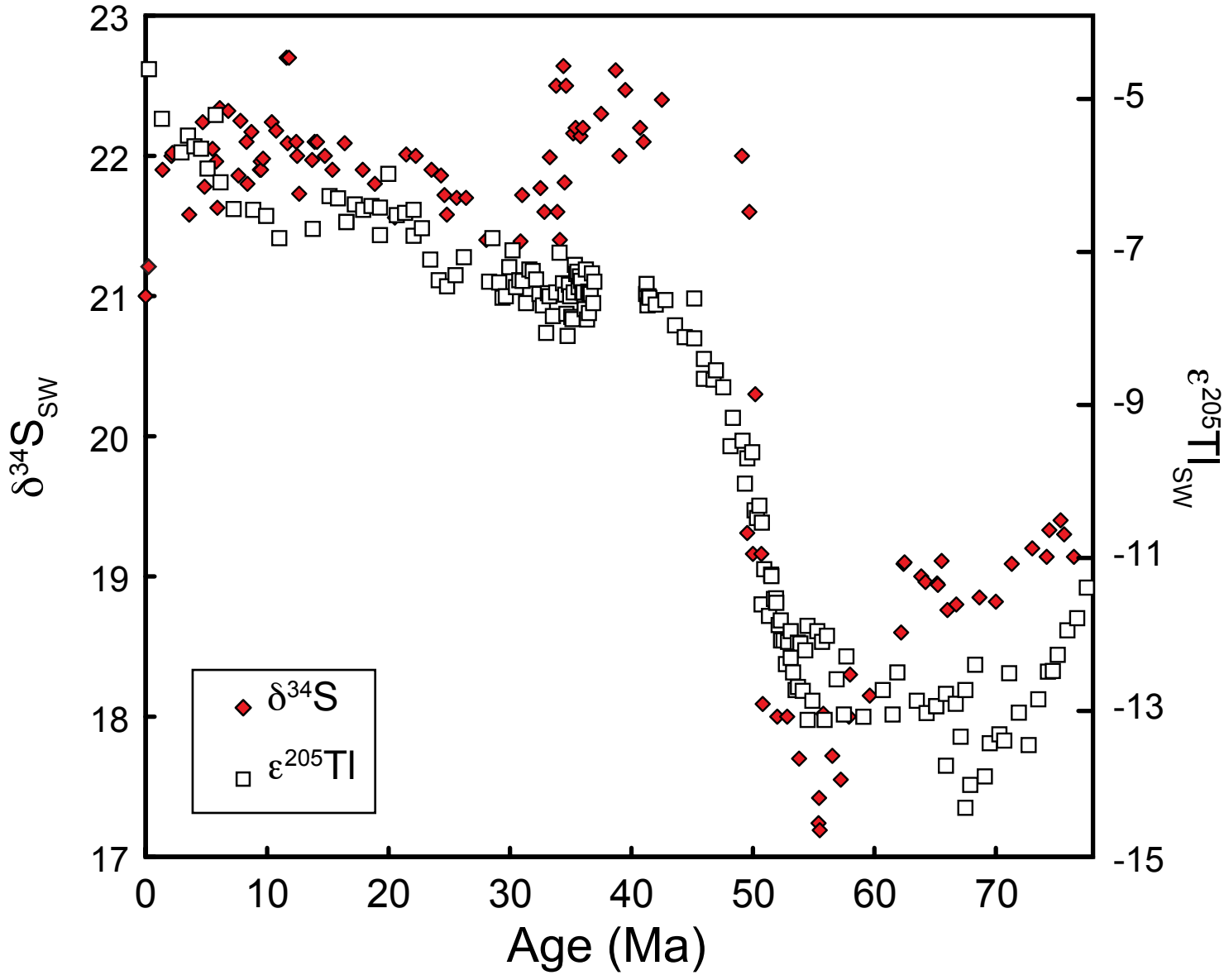
23
22
21
20
19
18
17
-5
-7
-9
-11
-13
-15
0
10
20
30
40
50
60
70
Age (Ma)
δ34SSW
ε205TlSW
δ34S
ε205Tl

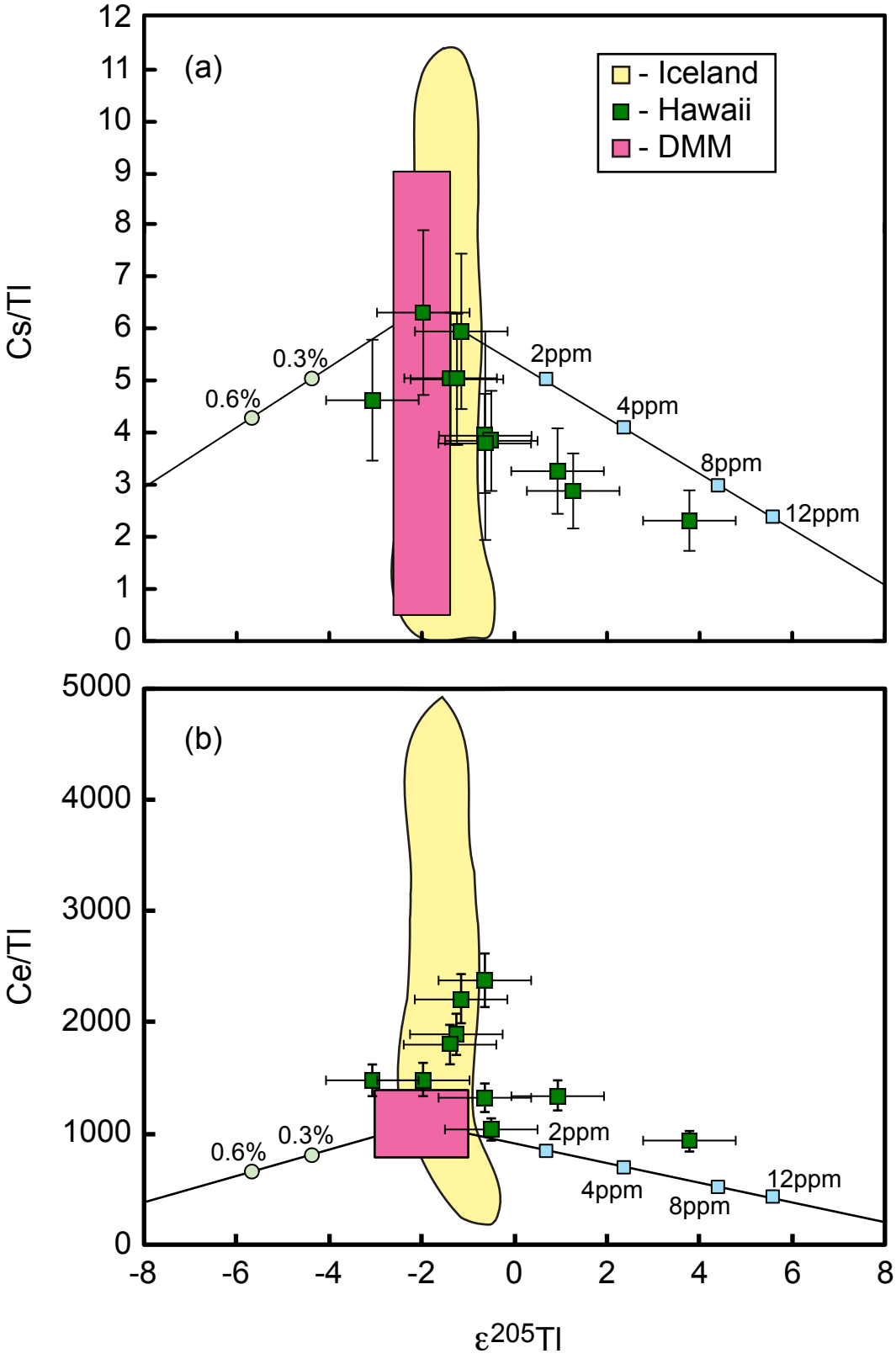
(a)
- Iceland
- Hawaii
- DMM
Cs/Tl
0.6%
0.3%
2ppm
4ppm
8ppm
12ppm
(b)
Ce/Tl
0.6%
0.3%
2ppm
4ppm
8ppm
12ppm
ε205Tl